Structure-Activity Relationship Studies of Strigolactone-Related Molecules for Branching Inhibition in Garden Pea: Molecule Design for Shoot Branching[1][W]

François-Didier Boyer*, Alexandre de Saint Germain, Jean-Paul Pillot, Jean-Bernard Pouvreau, Victor Xiao Chen, Suzanne Ramos, Arnaud Stévenin, Philippe Simier, Philippe Delavault, Jean-Marie Beau, and Catherine Rameau

Centre de Recherche de Gif, Institut de Chimie des Substances Naturelles, Unité Propre de Recherche 2301 Centre National de la Recherche Scientifique, F–91198 Gif-sur-Yvette cedex, France (F.-D.B., V.X.C., S.R., A.S., J.-M.B.); Unité Mixte de Recherche 1318 INRA-AgroParisTech, Institut Jean-Pierre Bourgin, F–78000 Versailles, France (A.d.S.G., J.-P.P., C.R.); and L'Université Nantes Angers Le Mans, Laboratoire de Biologie et Pathologie Végétales, Institut Fédératif de Recherche 149 Qualité et Santé du Végétal, EA 1157, 44322 Nantes cedex 3, France (J.-B.P., P.S., P.D.)

Initially known for their role in the rhizosphere in stimulating the seed germination of parasitic weeds such as the *Striga* and *Orobanche* species, and later as host recognition signals for arbuscular mycorrhizal fungi, strigolactones (SLs) were recently rediscovered as a new class of plant hormones involved in the control of shoot branching in plants. Herein, we report the synthesis of new SL analogs and, to our knowledge, the first study of SL structure-activity relationships for their hormonal activity in garden pea (*Pisum sativum*). Comparisons with their action for the germination of broomrape (*Phelipanche ramosa*) are also presented. The pea *rms1* SL-deficient mutant was used in a SL bioassay based on axillary bud length after direct SL application on the bud. This assay was compared with an assay where SLs were fed via the roots using hydroponics and with a molecular assay in which transcript levels of *BRANCHED1*, the pea homolog of the maize *TEOSINTE BRANCHED1* gene were quantified in axillary buds only 6 h after application of SLs. We have demonstrated that the presence of a Michael acceptor and a methylbutenolide or dimethylbutenolide motif in the same molecule is essential. It was established that the more active analog **23** with a dimethylbutenolide as the D-ring could be used to control the plant architecture without strongly favoring the germination of *P. ramosa* seeds. Bold numerals refer to numbers of compounds.

Strigolactones (SLs) represent the most recent class of hormones identified in plants for their role in repressing shoot branching. Their existence as a novel branching inhibitor signal was suggested through grafting experiments with high-branching mutants in pea (*Pisum sativum*; Beveridge et al., 1997; Beveridge, 2000) and in Arabidopsis (*Arabidopsis thaliana*; Turnbull et al., 2002; Booker et al., 2004). Analysis of the mutated genes indicated that some of them encode Carotenoid Cleavage Dioxygenase (CCD) enzymes, suggesting that the branching inhibitor was carotenoid derived (Sorefan et al., 2003; Booker et al., 2004; Matusova et al., 2005). When mutated in *CCD7* or *CCD8* genes, the plants were shown to be deficient in SLs. Treatment of these mutants by exogenous application of SLs inhibited the growth of lateral buds and restored the wild-type phenotype. Other branching mutants (*max2/rms4*) suspected to be affected in the hormone signaling pathway rather than in hormone synthesis were found to produce normal or higher amounts of SLs, and exogenous SL treatment did not suppress lateral bud growth. In the light of these data, some authors (Gomez-Roldan et al., 2008; Umehara et al., 2008; Domagalska and Leyser, 2011) concluded that SLs, or closely related molecules, were indeed the long-sought plant hormones that suppress lateral branch formation.

SLs have already been known as signaling molecules in the rhizosphere in both parasitic and symbiotic interactions. They were first identified in 1966 (Cook et al., 1966, 1972) as a seed germination stimulant of the parasitic weeds *Orobanche* and *Striga*, major agricultural pests around the Mediterranean Sea and in sub-Saharan Africa, respectively, where they constitute the major cause of crop damage. More recently, SLs have been shown to play a key role in the establishment of one of the most prevalent symbioses between the vast majority of land plants and arbuscular mycorrhizal (AM) fungi. SLs produced by plant roots stimulate spore germination and hyphal proliferation of AM fungi (Akiyama et al., 2005; Besserer et al., 2006). The hypothesis is that SLs boost their metabolism prior

[1] This work was supported by the Institut National de la Recherche Agronomique, Institut de Chimie des Substances Naturelles-Centre National de la Recherche Scientifique, and the Université de Nantes.

* Corresponding author; e-mail boyer@icsn.cnrs-gif.fr.

The author responsible for distribution of materials integral to the findings presented in this article in accordance with the policy described in the Instructions for Authors (www.plantphysiol.org) is: François-Didier Boyer (boyer@icsn.cnrs-gif.fr).

[W] The online version of this article contains Web-only data.

www.plantphysiol.org/cgi/doi/10.1104/pp.112.195826

to root colonization (Besserer et al., 2006). The AM symbiosis, which involves an ancient phylum of fungi, the Glomeromycota, arose very early in land plant evolution and is thought to have been instrumental in allowing successful plant colonization of the terrestrial environment (Simon et al., 1993). It has been proposed that the primary role of SLs was to attract these highly beneficial fungal symbionts, because of the parasitic plants having exploited this system much later to detect their host (Bouwmeester et al., 2007). SLs have also been shown to be synthesized by a nonvascular plant, the moss *Physcomitrella patens*, and to play a role in both chemical communication between plants and plant extension control (Proust et al., 2011). All these data suggest that SLs are very ancient molecules. Their role as interkingdom signaling molecules and between plants, together with their effect on shoot branching, constitute an intriguing plant signaling story.

To date, at least 15 naturally occurring SLs have been identified in root exudates of monocotyledonous and dicotyledonous plant species (Xie and Yoneyama, 2010), and most of them have been structurally characterized, very often with difficulties. It is expected that many others will be identified later (Yoneyama et al., 2009; Zwanenburg et al., 2009). Predominant SLs differ in identity in different species, although relatives tend to have similar SLs. SLs present a common four-cycle skeleton (A, B, C, and D), with cycles A and B bearing various substituents and cycles C and D being lactone heterocycles connected by an ether enol bond (Fig. 1). The first analysis of the distribution of SLs in different species suggests that 5-deoxystrigol is generally shared by both monocots and dicots, while orobanchol and orobanchyl acetate, for which structural revisions were recently proposed (Ueno et al., 2011b; Vurro and Yoneyama, 2012), seem to be found in dicots but not in monocots. Solanacol (Xie et al., 2007; Chen et al., 2010), identified in tobacco (*Nicotiana tabacum*), is the only SL having an aromatic A-ring. The highly active synthetic analog of strigol, known as GR24 and commonly used in biological experiments, also has an aromatic A-ring (Fig. 1). All currently known natural SLs possess the same CD rings with a methyl at the C4′ position, suggesting the importance of this structure for bioactivity. The identification of SLs is difficult partly because they are produced by plants in extremely low quantities and are relatively unstable. The level of the endogenous SL 2′-epi-5-deoxystrigol in rice (*Oryza sativa*) roots is about 20 pg g^{-1} fresh weight (Umehara et al., 2008), but SL levels found in roots and in root exudates are strongly dependent on nutrient availability, notably phosphorus and nitrogen (Yoneyama et al., 2007, 2012). SLs are inherently unstable in water, particularly at pH > 7, as this nucleophilic agent cleaves the enol ether bond between the C- and D-rings (Akiyama and Hayashi, 2006) to furnish the hydroxymethylbutenolide **3** (Fig. 2) and the formyl tricyclic lactone **6** (Fig. 3). These compounds and GR24 analogs have also been found to be light sensitive (Johnson et al., 1981). Activities of SLs could be detected at concentrations as low as 10^{-13} M on AM fungi (Akiyama and Hayashi, 2006), 10^{-12} M on seeds of parasitic weeds (Xie and Yoneyama, 2010), and 10^{-8} M for GR24 on lateral buds (Gomez-Roldan et al., 2008).

Most studies on the bioactivity of SLs investigated their action as a germination stimulant of parasitic seed weeds. The methyl substituent in the D-ring at C4′ is essential for bioactivity as a germination stimulant that underlines the importance of the D-ring (Zwanenburg et al., 2009). The presence of the 4-hydroxyl group seems to enhance the activity. It was recently reported that, generally, natural hydroxy-SLs are about 10- to 100-fold more active than their acetates on *Orobanche minor* and broomrape (*Phelipanche ramosa*) seed germination (Xie et al., 2008; Kim et al., 2010). The results are inverted for aromatic A-ring analogs of orobanchol for seeds of parasitic weeds (Malik et al., 2011). The C2′-(*R*) stereochemistry was also reported to be an important structural feature for potent germination stimulation activity for strigol, sorgolactone, orobanchol, orobanchyl acetate, and GR24 derivatives (Mangnus et al., 1992; Ueno et al., 2011a, 2011b). Recently, it was demonstrated that A-ring dimethyl substitution on GR24 lowers the germination activity (Malik et al., 2010). However, germination stimulation activity of SLs may be different from one parasitic plant species to another (Sato et al., 2005; Yoneyama et al., 2010; Ueno et al., 2011b). Structure-activity relationship (SAR) studies suggest that the CD ring moiety is the essential structure for stimulating seed germination (Zwanenburg et al., 2009). This CD structure unit was also proposed to be essential for AM fungi (Akiyama and Hayashi,

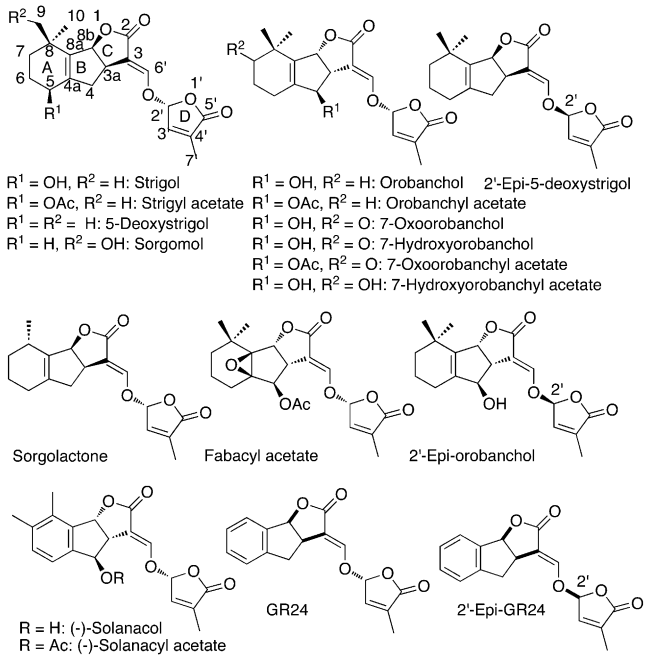

Figure 1. Natural SLs and analogs. Ac, Acetyl.

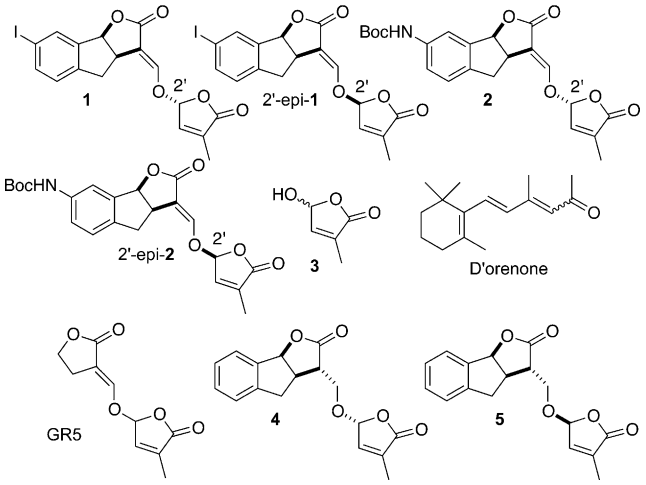

Figure 2. Known SL analogs and d'orenone. Boc, *t*-Butoxycarbonyl.

2006). Very recently, new data (Akiyama et al., 2010; Prandi et al., 2011) were made available concerning the hyphal branching activity. Structural requirements for this activity were reportedly very similar to those for germination stimulation of root parasites. However, the authors showed that the enol ether link between rings C and D can be replaced by an alkoxy or imino ether with little decrease in activity.

SL SAR studies are now required to define their role in repressing shoot branching. In this study, we used a branching bioassay developed with the pea SL-deficient mutant *rms1* to analyze the hormonal activity of various natural SLs and synthetic analogs. This biological assay was completed by a molecular assay using the pea *BRANCHED1* (*PsBRC1*) gene encoding a transcription factor of the plant-specific TCP family named from the first three identified members, the maize TEOSINTE BRANCHED1, CYCLOIDEA in *Antirrhinum majus*, and PCF-coding genes in rice. *PsBRC1* was shown to be transcriptionally up-regulated by SLs in axillary buds of the SL-deficient *rms1* mutant but not in the SL-response *rms4* mutant, indicating that it is involved in the SL-signaling pathway to repress branching (Braun et al., 2012). This work represents, to our knowledge, the first SAR study of SLs for their hormonal activity in branching inhibition. SAR studies were performed in parallel for activity on the germination of *P. ramosa*. An SL analog with strong activity for branching inhibition in pea (*Pisum sativum*) together with low activity for broomrape seed germination is revealed.

RESULTS

Synthesis of SL Analogs

The SL SAR for the inhibition of bud outgrowth can be established as for seed germination of parasitic plants (Zwanenburg et al., 2009) by simplifying the SL skeleton. The relevant question is whether the bioactiphore is the same as that for seed germination of parasitic plants or for hyphal proliferation of AM fungi.

Several natural SLs were tested along with the well-known GR24, in which the A-ring was replaced by an aromatic ring. Several GR24 analogs (**7**, **9**, **10**, **27**) lacking the D-ring were also synthesized (Fig. 3). Bold numerals refer to numbers of compounds. Reaction of tricycle **6** with benzylamine (dibenzylamine) furnished quantitatively under microwave irradiation the expected enamine **9** (**7**). The geometry of the enamine was determined by Nuclear Overhauser Enhancement Spectroscopy correlations observed between one

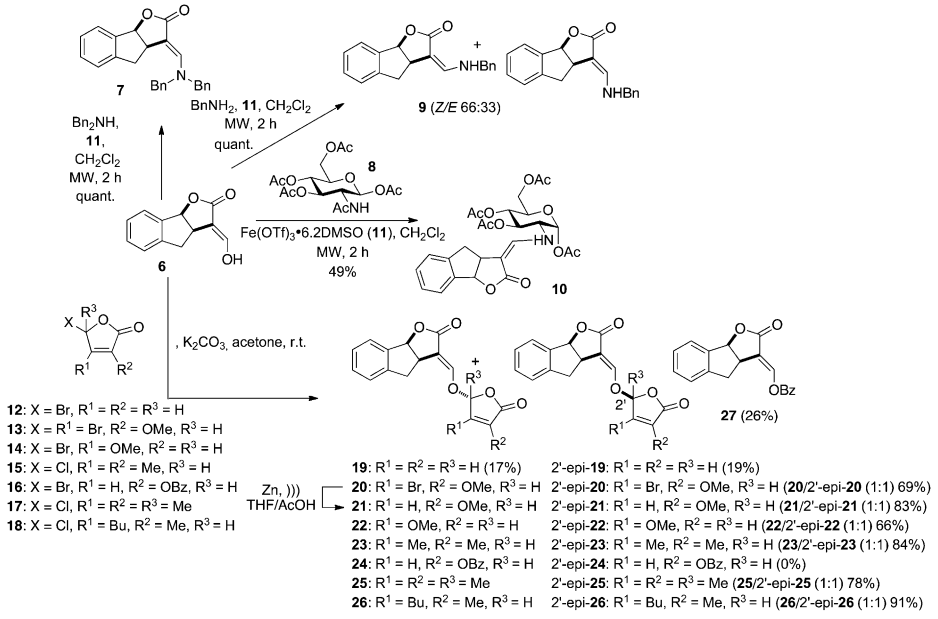

Figure 3. Synthesis of D-modified GR24 analogs. Ac, Acetyl; Bn, benzyl; Bu, *n*-butyl; Bz, benzoyl; Me, methyl; MW, microwave irradiation; r.t., room temperature; Tf, trifluoromethanesulfonyl.

benzylic methylene and H4 for **7** (only *E* geometry) and H6′ and H4 for the major *Z* isomer **9**, respectively. Enamine **10** was prepared by the reaction of tricycle **6** with the commercially available GlcNAc acetate **8** in the presence of anhydrous ferric triflate under microwave irradiation (Stévenin et al., 2012). The exclusive formation of the *Z* enamine **10** could be rationalized by the possible presence of a hydrogen bond between the NH and the oxygen atom at C2 in this geometry. This geometry was largely studied as in the case of the protection of the amino group of amino sugars by the acylvinyl group (Gomez-Sanchez et al., 1984) or the primary amine-labile vinylogous amide type-protecting group. Variations of the D-ring substituents were performed using D-ring precursors **12** to **18** for the coupling with enol **6**. In one case, the reaction with D-ring precursor **16** did not lead to the expected diastereoisomers **24/**2′-epi-**24** but to the transesterification product **27**, even with the solid/liquid conditions (K_2CO_3/acetone) known to avoid this side reaction (Hoffmann et al., 1989).

A racemic mixture of the AB-ring-truncated synthetic analog, GR5, was also prepared by a one-pot procedure involving the coupling of lactone with the suitable butenolide **32** (Macalpine et al., 1976) via an enol ether linkage (Fig. 4). The D analog of GR5 (**30**) was furnished from γ-butyrolactone, and the 3,4-dimethylbutenolide D-ring precursor **15** was easily obtained in bulk quantities (Canevet and Graff, 1978; Johnson et al., 1981). The influence of the replacement of the enol ether linkage by a thioenol ether and an enamine was also examined. Enamine **29** was obtained from the known 3-aminomethylenedihydrofuran-2-one **28** (Zanatta et al., 2003) by bis-alkylation with compound **15** in poor yield (8%). Preparations of **23/**2′-epi-**23** and SL mimic **31** were accomplished in the same way from enol **6** and commercially available 4-chlorobenzenethiol, respectively, in high (84% for **23/**2′-epi-**23**; Fig. 3) to moderate (51% for **31**; Fig. 4) yields. The bioisostere (**33**) of GR24 (Mangnus and Zwanenburg, 1992) was synthesized from enol **6** via treatment of the corresponding methoxymethylene derivative (Fig. 5) with sodium hydrosulfide in methanol (Just et al., 1976) to furnish the sodium thiolate directly alkylated with the 5-bromo-3-methyl-2(5*H*)-furanone (**32**). The analogs substituted at C2′ and C3′ GR24 analogs (**25/**2′-epi-**25**: $R^1 = R^2 = R^3 =$ Me) and (**26/**2′-epi-**26**: R^1 = Bu, R^2 = Me, R^3 = H) were furnished by the coupling of enol **6** with the corresponding chloro D-ring precursor (**17** or **18**) with good yields (78% for **25/**2′-epi-**25**, 91% for **26/**2′-epi-**26**; Fig. 3).

In order to examine the influence of the enol function at the C3C6′ position and that of the double bond of the D-ring on the biological activity, we synthesized derivatives **34** to **37** from 2′-epi-GR24 and derivative **38** from **5** (Fig. 6). Hydrogenation of 2′-epi-GR24 proceeded rapidly in ethyl acetate (EtOAc) in the presence of 10% palladium on carbon to give the completely reduced derivative **34** (two isomers), resulting from the concomitant hydrogenolysis of the benzylic carbon-oxygen bond. A time-controlled hydrogenation furnished the D-ring-reduced lactone **35** as a sole diastereoisomer in 54% yield. Similarly, hydrogenation of enone **5** led to bis-lactone **38** in 50% yield. The stereochemistry on the D-ring was proven by Nuclear Overhauser Enhancement Spectroscopy correlations observed between H4′ and H2′. Oxidation of 2′-epi-GR24 was performed regioselectively by the action of a diluted solution of dimethyl dioxirane to give a 7:3 mixture of epoxides **36** in high yield. Subsequent oxirane opening of **36** by methanol in an acidic medium led to alcohols **37** (7:3).

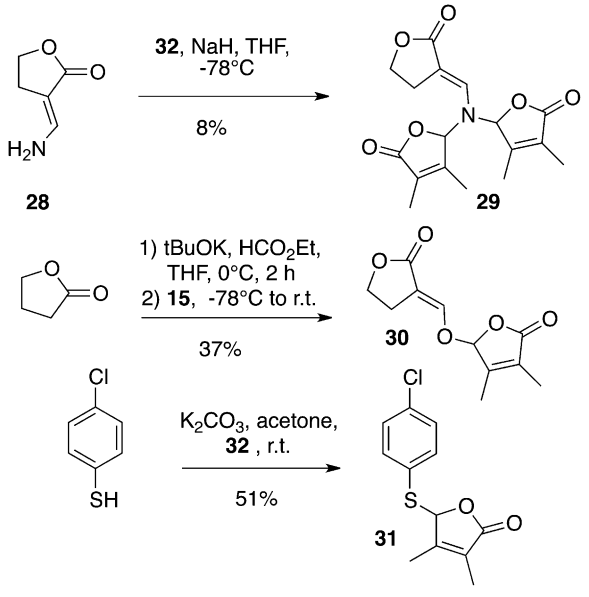

Figure 4. Synthesis of GR5 analogs and SL mimic **31**. Et, Ethyl; r.t., room temperature; tBu, *t*-butyl.

Biological Activities of SLs and Analogs

A simple bioassay was developed using the high-branching SL-deficient *rms1* mutant in garden pea to perform SAR studies on nine natural SLs and 33 analogs (structures are shown in Figs. 1–6) and to further clarify the structural requirements of this novel hormone in the control of shoot branching. Direct application of 10 μL of the solution to be tested on an axillary bud at a given node (generally node 3 or 4) was performed before its outgrowth, and the bud/branch length was measured 10 d later. The different compounds were first tested at a concentration of 1 μM and were considered inactive if no significant difference in the bud length was found compared with the mock control. For active compounds, lower concentrations were tested to analyze quantitative differences in bioactivity between molecules. Globally, when the treated bud was at node 3, its length was higher 10 d after treatment than when the treated bud was at node 4.

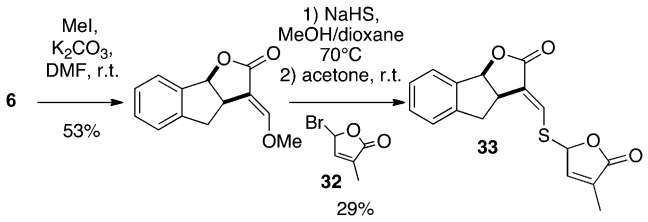

Figure 5. Synthesis of bioisostere **33** of GR24. DMF, Dimethylformamide; Me, methyl; r.t., room temperature.

Apolar SLs Are More Active Than Hydroxy-SLs

All tested natural SLs showed significant activities at a concentration of 1 μM (Table I). 5-Hydroxy-SL (strigol) and 4-hydroxy-SL (orobanchol; which was at the limit of significance in one experiment) showed less activity (Table I) than 5-acetate-SL (strigyl acetate) and 4-acetate-SL (orobanchyl acetate; e.g. at 500 nM, strigol was significantly less active than strigyl acetate [Kruskal-Wallis rank sum test, $P = 0.00047$]; Table I), as recently described for solanacol and solanacyl acetate (Chen et al., 2010). In all cases, acetate-SLs were always more active than their corresponding hydroxy-SLs, with the same dose-dependent activity for orobanchyl acetate, fabacyl acetate, and solanacyl acetate. 5-Deoxystrigol or sorgolactone without an oxygen function on the AB carbon bicycle presented high activity (Table I) better than the hydroxy-SLs (in Table I, compare 5-deoxystrigol and sorgolactone with strigol and orobanchol at 100 nM). In the case of fabacyl acetate, bud outgrowth inhibition activity was also found at the limit of significance at 10 nM (Table I). The best activity obtained with orobanchyl acetate and fabacyl acetate was in accordance with the fact that these SLs were identified in pea exudates (Gomez-Roldan et al., 2008; Xie et al., 2009). The activity differences between natural SLs observed in our bioassay may be attributed to the instability or low lipophilicity of the hydroxy-SLs, which may keep these molecules from reaching their putative receptors. We demonstrated that, in our conditions (ethanol/water), the acetate-SLs were more stable than the corresponding hydroxy-SLs (solanacol versus solanacyl acetate; Fig. 7A). D'orenone, mentioned as a putative intermediate in the SL biosynthesis pathway (Rani et al., 2008) until very recently (Alder et al., 2012), was also evaluated without success in bud outgrowth inhibition activity, even at 50 μM concentration (data not shown).

The Stereochemistry at C2′ and the Enantiomeric Purity Have a Low Effect on Bioactivity

The synthesis of (+)- and (−)-solanacol and the corresponding (+)- and (−)-solanacyl acetate allowed us to compare their bioactivity and to conclude that no significant difference was observed concerning each pair of enantiomers (Fig. 8; for solanacol, $P = 0.5601$ in one experiment and $P = 0.7028$ in another one; for solanacyl acetate, $P = 0.8$, Kruskal-Wallis rank sum test). Similarly, the stereochemistry at C2′ had little influence on the bioactivity of the solanacol series (solanacol versus 2′-epi-solanacol; Table I; $P = 0.148$ for 1 μM, Kruskal-Wallis rank sum test). These results were also demonstrated for GR24 (Table II) and compound **23** possessing dimethyl substitution at C3′ and C4′ (Fig. 9; no significant difference except in one experiment at 10 nM; Kruskal-Wallis rank sum test, $P = 2.358e\text{-}05$) and **2** bearing protected *t*-butoxycarbonylamino substituents at the C7 position on the A aromatic ring (Table III; $P = 0.3524$ and $P = 0.4518$ in two different experiments, Kruskal-Wallis rank sum test). However, for the derivative bearing an iodo group at C7 on the A aromatic ring, isomer **1** was found to be more active than isomer 2′-epi-**1** (Table III; $P = 0.00183$ and $P = 0.01842$ in two different experiments, Kruskal-Wallis rank sum test).

The ABC Part of the SL Backbone Can Be Removed without Affecting Bioactivity

SAR studies on synthetic SL analogs revealed that the activity of GR24, the well-known synthetic SL with an aromatic A-ring, as well as the more simple SL analog GR5 lacking A- and B-rings was similar to the most active natural SLs orobanchyl acetate, sorgolactone, and fabacyl acetate in the same concentration

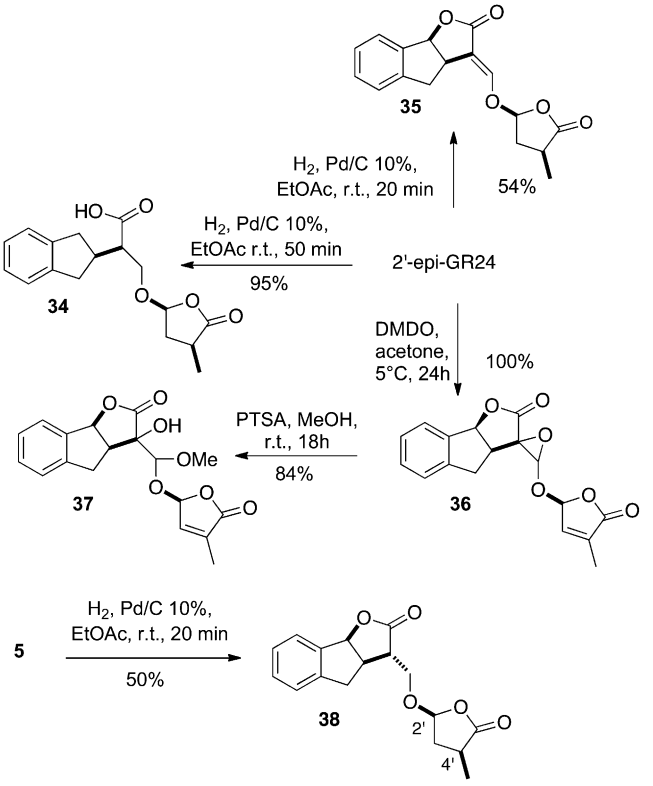

Figure 6. Synthesis of reduced and oxidized GR24 analogs. DMDO, Dimethyl dioxirane; Me, methyl; PTSA, *p*-toluenesulfonic acid; r.t., room temperature.

Table I. *Bud outgrowth inhibition activity assay results for natural SLs and derivatives*

P shows comparison of the SL treatment with the control treatment (0 nM) using the Kruskal-Wallis rank sum test.

Compound	Concentration	Length of Bud at Node 3 or 4 or 5 per Branch[a]	SE	*P*
		mm		
Strigol	1 μM	2.56[b]	0.22	1.138e-06
	500 nM	12.49[c]	2.22	0.04868
	500 nM	8.47[c]	2.81	0.8534
	100 nM	12.33[c]	2.52	0.09966
	100 nM	13.99[c]	3.39	0.6281
Strigyl acetate	1 μM	1.79[c]	0.21	2.827e-05
	500 nM	1.82[c]	0.21	0.0002111
	100 nM	7.38[c]	2.35	0.1297
5-Deoxystrigol	1 μM	2.28[b]	0.57	1.167e-07
	100 nM	3.99[c]	1.44	0.01491
Orobanchol	500 nM	5.49[c]	1.87	0.0005305
	100 nM	10.61[c]	2.40	0.02416
Orobanchyl acetate	500 nM	1.71[c]	0.16	0.001448
	500 nM	1.90[c]	0.23	0.0003437
	100 nM	2.92[c]	0.50	0.0003486
Sorgolactone	1 μM	1.65[b]	0.16	4.83e-08
	100 nM	2.32[c]	0.36	0.0005833
	100 nM	2.37[d]	0.23	0.001486
Fabacyl acetate	500 nM	1.69[c]	0.15	3.606e-05
	100 nM	2.52[c]	0.28	0.05819
	100 nM	1.62[c]	0.14	0.002244
	10 nM	2.08[c]	0.21	0.08477
	1 nM	2.41[c]	0.81	0.9616
(±)-Solanacol[e]	1 μM	6.87[c]	1.74	0.0992
	100 nM	7.66[c]	2.33	0.03308
(±)-2′-epi-Solanacol[e]	1 μM	6.87[c]	1.74	0.007101
	100 nM	14.53[c]	2.96	0.7473
(–)-Solanacol	1 μM	5.34[b]	1.20	1.64e-06
	1 μM	15.81[b]	4.19	0.006184
	1 μM	3.16[c]	0.58	0.00733
(+)-Solanacol	1 μM	4.34[b]	0.87	6.041e-06
	1 μM	9.58[b]	3.16	0.000638
	1 μM	4.68[b]	1.44	0.0381
(±)-Solanacyl acetate[e]	1 μM	1.59[c]	0.14	0.005552
	1 μM	1.59[c]	0.14	2.654e-05
	100 nM	3.87[c]	0.89	0.01044
	100 nM	3.13[c]	0.57	0.03405
	10 nM	6.26[c]	1.66	0.1213
	10 nM	2.40[c]	0.50	0.002546
	1 nM	12.13[c]	1.49	0.1518
(+)-Solanacyl acetate (1 μM)	1 μM	2.70[b]	0.39	3.19e-06
	1 μM	3.71[c]	1.04	0.03391
(–)-Solanacyl acetate (1 μM)	1 μM	5.57[b]	3.72	1.582e-05
	1 μM	1.90[c]	0.14	0.00176

[a]These data are means ± SE (n = 24), obtained 10 d after treatment. [b]Node 3. [c]Node 4. [d]Node 5. [e]Tested previously (Chen et al., 2010).

range (Tables I, II, and VI). In some experiments, GR5 was even more active when compared with GR24 at 10 nM (P = 0.0236, Kruskal-Wallis rank sum test) and at some nodes in hydroponics (see below; Supplemental Figs. S1 and S2), as demonstrated recently in rice (Yamaguchi et al., 2010). The SL mimic **31**, an analog of debranones (Fukui et al., 2011) with a 3,4-dimethylbutenolide D-ring and a 4-(chlorophenyl) thio group replacing the ABC part, also presented significant activity in branching repression at nanomolar concentrations (Table VI).

The D Part of the SL Backbone Attached to a Suitable Unsaturated System Is Essential for Bioactivity

The influence of the D-ring was established by the following results. The analogs of GR24, in which the enol ether group (>C = CH-O-) was replaced by an

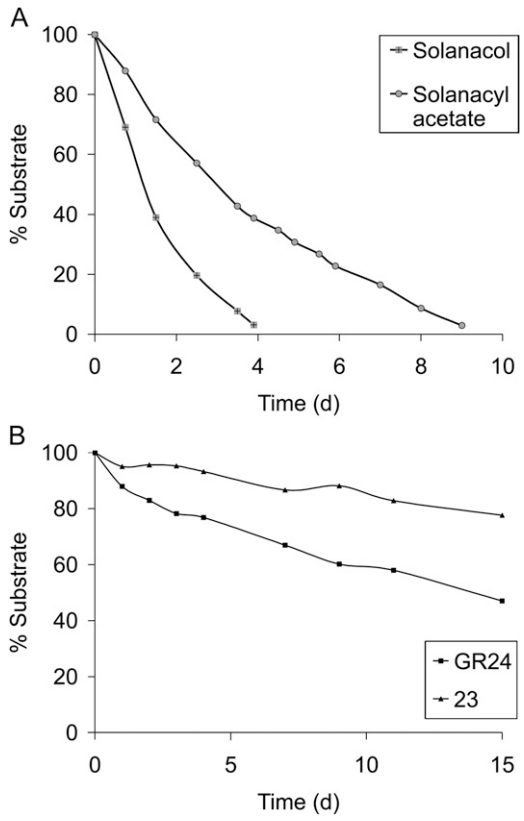

Figure 7. A, Chemical stability of solanacol and solanacyl acetate in a solution of ethanol:water (1:4, v/v) at 21°C (pH 6.7). B, Chemical stability of GR24 and **23** in a solution of ethanol:water (1:4, v/v) at 21°C (pH 6.7).

enamino group (>C = CH-N-) bearing either a benzyl (**7**, **9**) or a glucosyl (**10**) group (Fig. 3), were inactive at 1 μM concentration (Table IV). The D-ring precursor **3** was also found to be inactive, as was the combination of **3** with the ABC tricyclic derivative **6** or **27** (Table IV). Modifications of the substitution of the D-ring led to a drastic effect on bioactivity. Substitutions by a methoxy group at the C3′ or C4′ position (**20**–**22**) or lack of a methyl group (**19**) at the same positions led to an activity loss (Table IV). However, both compounds **23** and **31** possessing dimethyl substitution at C3′ and C4′ were more active than GR24 and its GR5 analog **30** (Tables IV and VI; Fig. 10; **23**/2′-epi-**23** were significantly more active than GR5 at 10 nM; Kruskal-Wallis rank sum test, $P = 0.01135$). This higher activity could be correlated with the relative high stability of **23** in aqueous medium in comparison with GR24 (Fig. 7B). The substitution at C2′ by a methyl group (**25**) or at C3′ by a butyl group (**26**) instead of a methyl group (**23**) significantly decreased bioactivity (Table IV). To study the influence of the double bonds at C3C6′ and C3′C4′, reduced and oxidized analogs of GR24 were evaluated. Completely reduced derivative **34**, 3,6′,3′,4′-tetrahydro-2′-epi-GR24 (**38**), and analogs with an oxidized enol ether group (**36**, **37**) were either inactive or only slightly active (Fig. 6; Table V). The very low activity of epoxide **36** could be explained by the fast degradation (less than 1 h) of this compound under the test conditions (acetone/ethanol/water) via the opening of the oxirane ring and cleavage of the D-ring (data not shown). Analogs **35** with a saturated D-ring and **5**, in which the carbon double bond in the CD-connecting enol ether was reduced to a single bond, presented significant activity (Table V) at micromolar concentrations but decreased rapidly as the concentration decreased. Finally, replacing the heteroatom attached at C6 by nitrogen or sulfur (**29**, **33**; Figs. 4 and 5) showed no activity for bud outgrowth inhibition (Tables V and VI).

Bioactivity of SLs When Applied via the Root System

To investigate the effects of the most active SL analogs (GR24, GR5) and analog **23** on shoot branching when provided via the roots, we developed a hydroponic culture system in which pea seedlings were placed 6 d after sowing (before leaf expansion at node 3). SLs were added at this stage into the culture solution, and branching at each node was observed 2 weeks later. In a first experiment (Supplemental Fig. S1), GR24 and GR5 were added at a final concentration of 3 μM. Bud outgrowth was significantly repressed at the upper nodes (nodes 3 and 4) by treatment with either or both SLs. In pea, the number of axillary buds per axil differed along the stem and was highest at node 2, where four buds could be found, with one being larger than the remainder (the accessory buds; Gould et al., 1987). At the basal nodes (nodes 1 and 2), two branches per node were generally observed for our SL-deficient *rms1* mutant line. The lengths of the different basal branches were measured and analyzed separately in the *rms1* mutant grown on the hydroponic system. A significant reduction of the bud/branch length was observed only for the second branch at both nodes for GR5 and only at

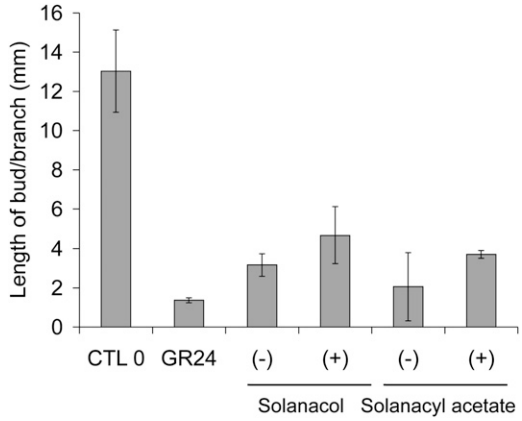

Figure 8. Activity of (+)- and (−)-solanacol and (+)- and (−)-solanacyl acetate. Lengths of axillary buds are shown at 10 d after direct application of a solution at 1 μM at node 4. Data are means ± SE ($n = 24$). CTL 0, Control 0.

Table II. *Bud outgrowth inhibition activity assay results for GR24 analogs: influence of the stereochemistry at C2′*

P shows comparison of the SL treatment with the control treatment (0 nM) using the Kruskal-Wallis rank sum test.

Compound	Concentration	Length of Bud at Node 3 or 4 or 5 per Branch[a]	SE	*P*
		mm		
GR24/2′-epi-GR24	(1:1) 1 μM	1.13[b]	0.06	0.0001434
GR24	1 μM	1.81[c]	0.17	3.658e-08
	1 μM	2.32[c]	0.21	7.703e-07
	1 μM	3.16[c]	1.03	3.123e-07
	1 μM	5.02[c]	1.08	0.0002323
	1 μM	5.58[c]	2.29	3.431e-07
	1 μM	1.37[b]	0.13	1.814e-05
	1 μM	1.38[b]	0.15	0.00296
	1 μM	1.39[b]	0.09	0.01278
	1 μM	1.54[b]	0.09	2.246e-05
	1 μM	1.80[b]	0.21	0.002495
	500 nM	1.40[b]	0.18	0.00419
	500 nM	1.69[b]	0.18	2.733e-05
	500 nM	1.89[b]	0.29	0.001434
	500 nM	5.48[b]	1.85	0.0006748
	100 nM	1.87[c]	0.13	5.42e-08
	100 nM	4.39[c]	0.38	1.598e-07
	100 nM	7.26[c]	1.75	0.001085
	100 nM	16.78[c]	3.76	0.001103
	100 nM	1.44[b]	0.06	6.515e-07
	100 nM	1.57[b]	0.13	0.001664
	100 nM	1.66[b]	0.13	7.789e-05
	100 nM	3.15[b]	1.10	0.006062
	100 nM	3.65[b]	1.88	0.0007414
	100 nM	3.74[b]	1.59	0.0001373
	100 nM	3.74[b]	0.82	0.001448
	100 nM	4.83[b]	1.50	0.0004835
	100 nM	6.56[b]	2.89	0.002068
	100 nM	1.87[d]	0.24	0.0007518
	10 nM	14.05[c]	1.79	0.1837
	10 nM	14.99[c]	2.39	0.2825
	10 nM	28.74[c]	3.46	0.1188
	10 nM	1.76[b]	0.12	2.011e-05
	10 nM	1.90[b]	0.24	0.03709
	10 nM	3.93[b]	1.53	0.003062
	10 nM	11.85[b]	2.24	0.942
	1 nM	8.42[c]	1.66	0.006272
	1 nM	19.53[c]	0.87	0.4435
	1 nM	2.22[b]	0.22	0.003631
	1 nM	3.36[b]	0.70	0.6577
	0.1 nM	3.87[b]	0.28	0.42
	0.01 nM	16.32[c]	1.28	0.1518
2′-epi-GR24	1 μM	1.23[b]	0.08	0.0008346
23	1 μM	1.80[c]	0.11	7.656e-08
	1 μM	1.96[c]	0.13	3.804e-08
	100 nM	1.49[c]	0.07	1.217e-07
	100 nM	1.67[c]	0.14	5.061e-08
	100 nM	1.78[c]	0.09	9.488e-09
	100 nM	1.82[c]	0.11	1.55e-05
	100 nM	2.01[c]	0.13	1.344e-08
	100 nM	2.14[c]	0.16	1.29e-06
	100 nM	2.44[c]	0.47	1.637e-05
	10 nM	1.66[c]	0.13	2.952e-06
	10 nM	2.13[c]	0.13	8.939e-09
	10 nM	2.81[c]	0.49	9.998e-06
	10 nM	3.06[c]	0.74	4.543e-05

(*Table continues on following page.*)

Table II. (*Continued from previous page.*)

Compound	Concentration	Length of Bud at Node 3 or 4 or 5 per Branch[a]	SE	*P*
	10 nM	8.81[c]	3.11	4.398e-05
	1 nM	4.43[c]	0.83	2.531e-07
	1 nM	7.27[c]	1.61	0.003078
	1 nM	11.94[c]	1.93	0.5845
	1 nM	13.88[c]	3.83	0.007361
	0.1 nM	18.70[c]	1.44	0.1024
	0.1 nM	28.65[c]	3.65	0.9561
	0.1 nM	2.63[b]	0.16	0.04531
	0.01 nM	11.75[c]	1.45	0.0814
2′-epi-**23**	100 nM	1.79[c]	0.13	3.919e-05
	100 nM	1.76[c]	0.23	7.853e-07
	10 nM	1.84[c]	0.11	1.931e-05
	10 nM	1.66[c]	0.13	2.952e-06
	1 nM	11.36[c]	2.57	0.386
	0.1 nM	18.70[c]	1.44	0.1024

[a]These data are means ± SE (n = 24), obtained 10 d after treatment. [b]Node 4. [c]Node 3. [d]Node 5.

node 1 for GR24 (Supplemental Fig. S1). In a second experiment, GR24 and **23** were added at a final concentration of 1 μM. At the upper nodes, both SLs significantly repressed bud outgrowth. At the basal nodes, GR24 and **23** significantly reduced the branch length of the second one at both nodes (Fig. 11). Compound **23** also significantly reduced the growth of the main branch at node 1. To summarize, experiments with the hydroponic culture in which SLs were applied via the root system confirmed the results obtained with direct application onto the axillary bud, where GR5 and especially compound **23** showed higher bioactivity than did GR24 for branching inhibition.

A Molecular Assay Using PsBRC1 Transcript Levels

The transcript level of *PsBRC1* was reduced in the axillary buds of SL-deficient mutants in comparison with the wild type (Braun et al., 2012). This gene, mostly expressed in the axillary bud, is transcriptionally up-regulated by SLs without the requirement of protein synthesis, and its transcript level in the axillary bud correlates with the observed bud growth responses in the SL-deficient *rms1* mutant (Braun et al., 2012; Dun et al., 2012). The activity of solanacol and solanacyl acetate, which showed a quantitative difference in bioactivity for bud outgrowth inhibition, was tested at the molecular level. Their effects on the *PsBRC1* transcript level were quantified using real-time PCR in *rms1* axillary buds 6 h after direct application of GR24, solanacol, and solanacyl acetate at a concentration of 1 μM. Bud length was measured 10 d after SL application to ensure their activity in this experiment (Fig. 12A). In comparison with the control without SL, at 1 μM, the three SLs induced a significant increase in *PsBRC1* expression (Fig. 12B). At 500 nM, only GR24 and solanacyl acetate induced significant increases in *PsBRC1* expression (Supplemental Fig. S3). At 1 μM, solanacyl acetate triggered a higher *PsBRC1* expression than solanacol and GR24 (Fig. 12B). Consequently, phenotypic and molecular assays were in agreement for the branching control test of SLs, but differences were observed between assays. Solanacyl acetate showed higher activity than did GR24 according to the molecular assay, whereas both SLs showed the same activity in the branching assay.

Germination Stimulation Activity

The germination stimulatory activity of natural SLs and analogs was extensively studied in the past with a range of one-half-maximal effective concentration (EC_{50}) values (10^{-10} to 10^{-15} M) varying according to the root parasitic plants (*Orobanche*, *Striga*; Kim et al., 2010; Malik et al., 2011). In this study, the EC_{50} of each compound was determined with a range of concentrations tested between 10^{-16} and 10^{-4} M and the maximum percentage of germination. EC_{50} reflects the affinity of the compounds to the putative receptor over the effectiveness of the response induced. No significant

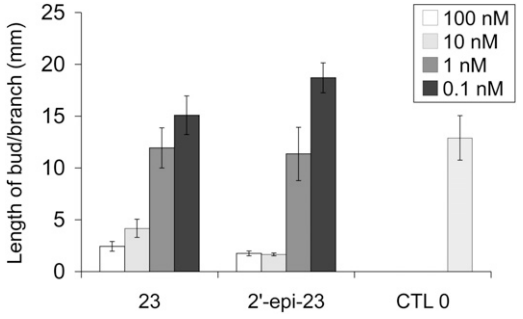

Figure 9. Comparative activity of SL analogs **23** and 2′-epi-**23.** Lengths of axillary buds are shown at 10 d after direct application at node 3. Data are means ± SE (n = 24). CTL 0, Control 0.

Table III. *Bud outgrowth inhibition activity assay results for GR24 analogs: influence of the substitution on the A-ring*

P shows comparison of the SL treatment with the control treatment (0 nM) using the Kruskal-Wallis rank sum test.

Compound	Concentration	Length of Bud at Node 3 or 4 per Branch[a]	SE	*P*
		mm		
1	1 μM	2.55[b]	0.20	5.113e-07
	1 μM	1.68[c]	0.16	1.304e-05
	500 nM	3.93[b]	1.06	2.996e-06
	100 nM	4.28[c]	1.16	5.272e-05
2′-epi-**1**	1 μM	4.80[b]	0.93	4.339e-06
	1 μM	7.24[c]	2.46	0.02181
2	1 μM	4.09[c]	1.74	0.1266
	500 nM	2.20[c]	0.26	0.08286
2′-epi-**2**	1 μM	2.90[c]	1.10	0.3367
	500 nM	4.90[c]	2.80	0.1185

[a]These data are means ± SE (n = 24), obtained 10 d after treatment. [b]Node 3. [c]Node 4.

difference was observed for the maximum germination percentage (from 94% ± 4% to 96% ± 3%) obtained between the different SLs (ANOVA, $P < 0.05$). Activities of SLs were then compared using their EC_{50}. The most potent compounds for branching inhibition (GR24, GR5, **23**) were examined for their activity on seed germination in comparison with other SL analogs. Seeds of *P. ramosa* were used, and in our hands, the best activity was observed for GR24 (EC_{50} ± SE = $3.4 \times 10^{-12} \pm 2.1 \times 10^{-12}$ mol L^{-1}; Fig. 13). The stereochemistry at C2′ had no significant influence on the bioactivity in the GR24 series (GR24 versus 2′-epi-GR24, $3.4 \times 10^{-12} \pm 1.18 \times 10^{-12}$ and $2.13 \times 10^{-12} \pm 1.18 \times 10^{-12}$ mol L^{-1}, respectively; Student's t test, $P < 0.05$; Fig. 13). As already

Table IV. *Bud outgrowth inhibition activity assay results for GR24 analogs: influence of the D-ring*

P shows comparison of the SL treatment with the control treatment (0 nM) using the Kruskal-Wallis rank sum test.

Compound	Concentration	Length of Bud at Node 3 or 4 per Branch[a]	SE	*P*
		mm		
3	1 μM	32.09[b]	6.00	0.9167
6	500 nM	21.32[c]	2.67	0.7579
6/3	(1:1) 500 nM	19.55[c]	3.68	0.9019
7	1 μM	18.38[b]	1.03	0.195
9	1 μM	19.63[b]	0.86	0.6184
10	1 μM	17.89[b]	1.53	0.4226
27/3	(1:1) 1 μM	29.81[b]	3.69	0.2461
19	1 μM	6.82[c]	2.53	0.9097
20/2′-epi-**20**	(1:1) 1 μM	6.58[c]	2.16	0.7445
21	1 μM	18.09[b]	0.11	0.2672
22/2′-epi-**22**	(1:1) 1 μM	17.56[b]	1.52	0.1478
23/2′-epi-**23**	(1:1) 1 μM	2.67[b]	0.19	1.895e-08
	(1:1) 1 μM	2.55[b]	0.28	4.191e-06
	(1:1) 100 nM	3.22[b]	0.29	4.328e-08
	1:1) 100 nM	1.81[b]	0.12	5.225e-06
	(1:1) 10 nM	3.46[b]	0.34	3.937e-08
	1:1) 10 nM	1.89[b]	0.14	1.233e-05
	(1:1) 1 nM	8.31[b]	2.32	0.0247
	1:1) 1 nM	4.37[b]	1.19	0.0002118
	(1:1) 0.1 nM	8.07[b]	1.50	0.03062
25/2′-epi-**25**	(1:1) 1 μM	14.90[b]	4.14	0.09312
26/2′-epi-**26**	(1:1) 1 μM	6.57[b]	2.53	0.0002661

[a]These data are means ± SE (n = 24), obtained 10 d after treatment. [b]Node 3. [c]Node 4.

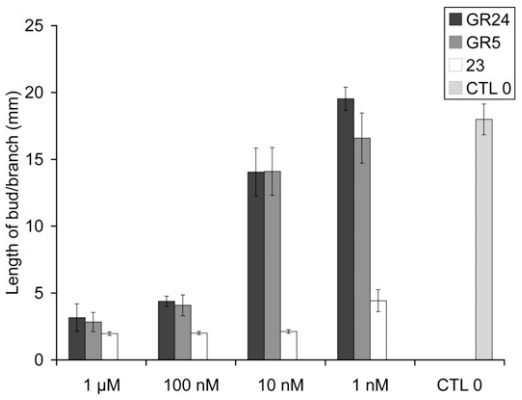

Figure 10. Dose-dependent activity of the most active SL analogs GR24, GR5, and **23** for branching inhibition. Lengths of axillary buds are shown at 10 d after direct application at node 3. Data are means ± SE (n = 24). CTL 0, Control 0.

described (Johnson et al., 1981), GR5 analogs (Table VII) were less active than their corresponding GR24 analogs (about 10- to 1,000-fold). Interestingly, analog **23** presented moderate activity in comparison with GR5 or GR24 (about 100 and 10,000 times less active, respectively; Supplemental Fig. S4). The reduced analogs of GR24 at C3C6′ positions (**4** and **5**) and the reduced analog **35** at C3′C4′ presented, in our study, moderate and good activity for the germination of *P. ramosa*, respectively (Fig. 13). In contrast, these compounds showed no activity on *Striga hermonthica* and *Orobanche crenata* seed germination (Mangnus and Zwanenburg, 1992).

DISCUSSION

Pea Branching Assays

Few SLs were tested for shoot branching inhibition so far (Gomez-Roldan et al., 2008; Umehara et al., 2008; Chen et al., 2010), not only because the hormonal function of SLs was discovered a few years ago but also because of the difficulty of the treatment and the relatively large amount of samples required in some species such as rice, where a hydroponic culture has to be used (Umehara et al., 2008; Fukui et al., 2011). In this SAR study, in which 42 molecules were tested, often with different concentrations, pea was proven to be an excellent model. Its simple architecture is particularly suitable for exogenous hormone applications, and access to axillary buds is very easy. One major advantage of our bioassay with direct bud application is the small quantity (less than 1 mg) of molecule needed. Using this assay, the most active compounds showed a significant activity at a concentration of 10 nM. Notable activities at 1 nM were also observed for **23**/2′-epi-**23** and **31** in some experiments. These results indicate a highly sensitive perception system for SL and a particularly potent activity as demonstrated for AM fungi (Akiyama and Hayashi, 2006) and for seed germination (Xie and Yoneyama, 2010). Certain molecules may be applied through the roots for several days using a hydroponic system, and their effect on branching at several nodes can be analyzed. Using this system, response differences between buds depending on their positions on the stem or between buds at basal nodes were shown. The SLs tested with hydroponics (GR24, GR5, **23**) were able to reduce branch lengths at

Table V. *Bud outgrowth inhibition activity assay results for GR24 analogs: influence of the double bonds at C3C6′ and C3′C4′ and influence of the nature of the heteroatom between C and D*

P shows comparison of the SL treatment with the control treatment (0 nM) using the Kruskal-Wallis rank sum test.

Compound	Concentration	Length of Bud at Node 3 or 4 per Branch[a]	SE	*P*
		mm		
34	1 µM	15.64[b]	1.49	0.02134
	1 µM	7.28[c]	2.62	0.6719
35	1 µM	8.34[b]	1.53	0.0001411
	500 nM	2.20[c]	0.16	0.1321
	500 nM	2.10[c]	0.10	0.07155
	100 nM	11.83[c]	3.08	0.3319
36	1 µM	17.15[c]	4.24	0.1831
	1 µM	10.22[b]	1.84	0.0003181
37	1 µM	17.13[b]	1.29	0.1482
	1 µM	5.53[c]	2.71	0.1932
4	1 µM	4.15[c]	0.83	0.08025
5	1 µM	5.55[b]	1.35	9.923e-06
	1 µM	11.38[b]	2.60	0.01761
	1 µM	1.87[c]	0.15	0.0002597
	500 nM	1.47[c]	0.08	0.008959
	100 nM	18.23[b]	2.45	0.5782
38	1 µM	9.07[b]	1.72	0.001774
33	1 µM	25.20[b]	4.74	0.162

[a]These data are means ± SE (n = 24), obtained 10 d after treatment. [b]Node 3. [c]Node 4.

Table VI. *Bud outgrowth inhibition activity assay results for GR5 analogs and SL mimic **31***

P shows comparison of the SL treatment with the control treatment (0 nM) using the Kruskal-Wallis rank sum test.

Compound	Concentration	Length of Bud at Node 3 or 4 per Branch[a]	SE	*P*
		mm		
GR5	1 μM	2.76[b]	0.27	3.842e-06
	1 μM	2.84[b]	0.71	6.845e-08
	1 μM	3.45[b]	0.31	2.456e-08
	100 nM	2.29[b]	0.26	3.78e-05
	100 nM	4.08[b]	0.77	1.373e-07
	100 nM	6.46[b]	1.25	0.0003009
	100 nM	16.78[b]	4.70	0.002689
	100 nM	1.58[c]	0.15	1.773e-05
	100 nM	1.87[c]	0.10	0.002514
	10 nM	6.88[b]	2.56	0.0006954
	10 nM	13.70[b]	2.05	0.08664
	10 nM	14.10[b]	1.79	0.1228
	10 nM	28.35[b]	4.40	0.3172
	10 nM	5.15[c]	1.85	0.03928
	1 nM	16.59[b]	1.88	0.7095
	1 nM	8.16[c]	2.12	0.5715
29	1 μM	24.17[b]	4.19	0.06404
30	1 μM	2.60[b]	0.50	9.502e-08
	100 nM	6.15[b]	1.29	5.678e-06
	10 nM	11.24[b]	1.64	0.001544
	1 nM	17.30[b]	1.48	0.6843
31	1 μM	1.81[b]	0.11	8.726e-08
	1 μM	2.05[b]	0.12	5.012e-07
	100 nM	2.00[b]	0.11	1.348e-07
	100 nM	2.36[b]	0.17	5.494e-06
	100 nM	1.56[c]	0.06	1.032e-07
	10 nM	2.43[c]	0.30	2.303e-06
	10 nM	1.65[c]	0.07	8.542e-07
	1 nM	8.28[b]	1.28	0.0003896
	1 nM	1.91[c]	0.21	0.0002094
	0.1 nM	3.02[c]	0.36	0.1417
	0.01 nM	17.24[b]	1.42	0.11

[a]These data are means ± SE (n = 24), obtained 10 d after treatment. [b]Node 3. [c]Node 4.

all nodes except for those at basal nodes (nodes 1 and 2), where only the small branch was inhibited. At these particular nodes, corresponding to scale leaves, the SL-deficient *rms1* mutant displayed two branches. Here, we found that even the most active SL was not able to reduce the main branch at node 2. At node 1, only **23** significantly reduced the growth of the main branch. In pea, wild-type lines often displayed one strong basal branching at nodes 1 and 2, suggesting that even endogenous SLs are not able to inhibit outgrowth of the main axillary bud at these nodes while axillary buds at upper nodes and accessory buds at basal nodes are inhibited. Consequently, the use of synthetic SL analogs to control shoot architecture may not be efficient to repress branching for all buds according to their positions along the stem. Two (nonexclusive) hypotheses are currently proposed for the action of SL to repress branching: (1) a direct and local action in the bud via *PsBRC1* (Braun et al., 2012); (2) a systemic action by dampening auxin transport and enhancing competition between shoot branches (Crawford et al., 2010). The fact that at basal nodes, where more than two buds are present, SL treatment generally inhibits the small branch while the strongest one is not inhibited could suggest that SL treatment increases the competition between the two branches at these nodes. Nevertheless, here, we show that the most active SL, **23**, is able to significantly inhibit the outgrowth/growth of both branches at node 1. This basal branching can also be inhibited by direct application of GR24 at high concentrations (e.g. 2 μM; Brewer et al., 2009), whereas only one application of GR24 at 100 nM is enough to inhibit axillary bud outgrowth at nodes 3 and 4. This is why we chose these nodes for our bioassay. Consequently, according to its position along the stem, the axillary bud will be more or less responsive to a local SL treatment or via the vascular stream. Because *PsBRC1* integrates SL and cytokinin signals that act antagonistically to regulate bud outgrowth (Braun et al., 2012), it is also possible that the cytokinin response may

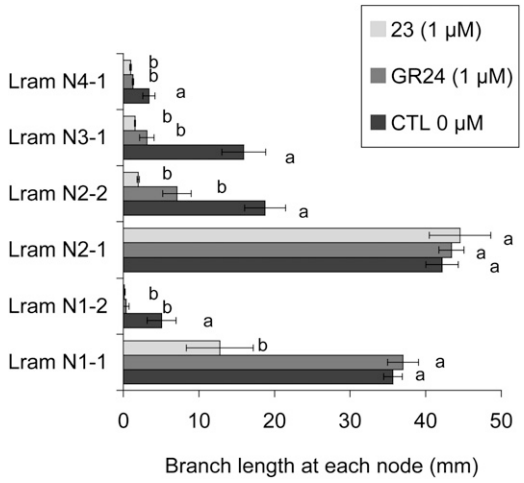

Figure 11. Bioassay on bud outgrowth using hydroponic culture. A comparison of the activity of GR24 and **23** at 1 μM is shown. Axillary bud lengths are shown at each node of *rms1* plants 2 weeks after treatment. Lram Ni-j, Ramification length at node i. j = 1 means the main branch at this node, and j = 2 means the second branch at this node when visible. Data are means ± SE (n = 12). Values that have the same letter (a or b) are not significantly different at P = 0.05. CTL 0, Control 0.

explain the difference in bud outgrowth potential according to its position on the stem.

Analysis of transcript levels of *PsBRC1* in a molecular assay was carried out to compare two SLs showing quantitatively different activities in our branching assay. Our results suggest that this molecular assay could be applied to test and compare the hormonal activity of SL analogs, particularly molecules with relatively low stability. This assay is based on transcript levels 6 h after SL application, whereas in the branching assay it is not clear how long the molecule needed to be active to repress bud outgrowth. This molecular assay could be used to investigate the lipophilicity of molecules and the penetration rate of the molecule in the tissue.

It is very likely that the activity for branching inhibition of the tested molecules is not toxicity. In our bioassay, when buds are "killed," their color changes from green to white/yellow. To confirm the activity of the molecule in branching inhibition and to discriminate from a possible toxicity, the molecule could be tested on a SL response mutant (e.g. *rms4*). In the case of toxicity, branching inhibition should also be observed in this mutant, whereas if the molecule is active using the *rms1* SL-deficient mutant, the same molecule should not inhibit bud outgrowth in *rms4*.

SL Structural Requirements for Repressing Branching

One major breakthrough in the discovery of SLs as a plant hormone can be seen in the study by Matusova et al. (2005) showing that SLs were derived from the carotenoid pathway. A SL biosynthesis scheme from β-carotene was proposed with olefin bond cleavage by CCD as a first step leading to the putative intermediate d'orenone, followed by several steps of reductions, allylic alcohol rearrangement, oxidation, allylic isomerizations, cyclizations, and coupling of the ABC intermediate with the D-ring precursor (Rani et al., 2008). From 5-deoxystrigol and 2′-epi-5-deoxystrigol, which may be common in many plants, further hydroxylations could lead to hydroxy-SLs and further acetylation to acetate-SLs. D'orenone was inactive in our conditions, demonstrating that this putative precursor could not be transformed to the active compound in the bud. Accordingly, a new biosynthesis scheme was proposed very recently (Alder et al., 2012) where trans-β-carotene is isomerized and then cleaved by CCD7 and CCD8 to give carlactone, a compound possessing A- and D-rings and the enol ether bridge, before being transformed in 5-deoxystrigol.

All nine natural SLs tested were active for branching inhibition, but with a quantitative difference in activity. Some synthetic SLs were as active as various natural SLs in the same range of concentrations (10^{-6} to 10^{-9} M), in which analog **23** was even more active. It appeared that lipophilicity is a major factor of the activity of natural SLs, since the hydrophobic natural SLs (5-deoxystrigol, sorgolactone, acetate-SLs) tested were more active in our bioassays than the hydroxy-SLs (strigol, orobanchol, solanacol).

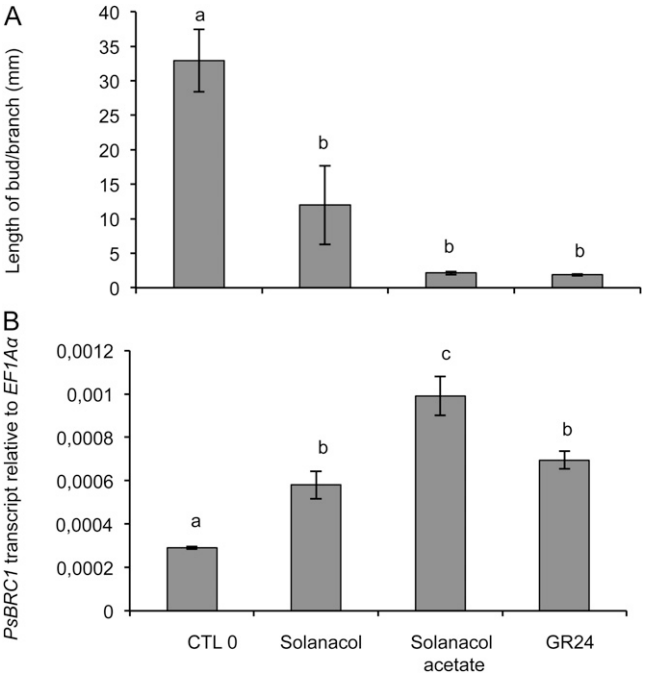

Figure 12. Effect of different SLs (1 μM) on *PsBRC1* transcript levels in axillary buds at node 3 of *rms1* plants. Plants were treated by direct application on the bud. A, Length of the axillary bud 10 d after treatment at node 3. Data are means ± SE (n = 12). B, *PsBRC1* transcript levels in the axillary bud 6 h after treatment. Data are means ± SE (n = 3 pools of 30 plants). Values that have the same letter (a–c) are not significantly different at P = 0.05. CTL 0, Control 0.

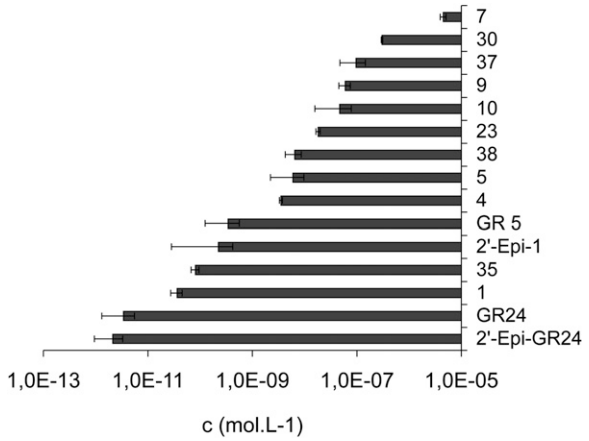

Figure 13. EC_{50} (mol L^{-1}) of various SL analogs toward *P. ramosa* seed germination.

All natural SLs identified so far from various plants bear invariant lactone heterocycles C and D, being connected by an ether enol bond. The SL structural requirements for shoot branching inhibition were demonstrated to be essential in this part of the molecule. Small modifications in this moiety of SLs led to drastic consequences on the bioactivity. If replacements of the carbon-carbon double bond at C3C6′or C3′C4′ and substitution at C2′ led to a significant reduction of the bioactivity, the addition of methyl at C3′ led to the very active compound **23** studied here. These results suggest that the D-ring is essential for bioactivity and that a small substitution at C3′ could modulate the interaction with the putative receptor and/or favor the formation of the active compound. The modifications on the AB part were not sufficient to substantially increase or decrease bioactivity. Similarly, the stereochemistry at C2′ or the absolute configuration had no effect on the bioactivity. The SAR of synthetic SLs showed that the ABC hydrophobic skeleton was not essential for the bud outgrowth inhibition activity and could easily be replaced by only the C-ring. These observations were also recently demonstrated in rice (Fukui et al., 2011), where debranones possessing only the D-ring connected to an aromatic cycle without the ABC part presented similar activity to GR24.

We could speculate that one of the functions of the ABC part is to provide a hydrophobic tail to facilitate the transport of SLs toward a putative receptor and influence the stability of the molecule. It is suggested that the SL instability is essential for their role in the rhizosphere as signaling the proximity of a host root to fungi and parasitic seeds (Parniske, 2008). *Orobanche* and *Striga* plants as well as AM fungi are obligate biotrophs and must colonize plant roots to obtain reduced carbon and to complete their life cycle. A steep SL concentration gradient may result from this instability, and spores and seeds will germinate only when located close to the host root. Whether this instability would also be essential for their hormonal role in the shoot is unlikely. The active branching inhibitor may not be one of the known SLs, and the SLs identified to date may only be the precursors. This hypothesis was proposed with the characterization of the dwarf and high-tillering rice *d14* mutant and the cloning of the rice *D14* gene encoding a protein of the α/β-hydrolase superfamily. D14 was suggested to act either at a later step of the active branching inhibitor biosynthesis or in its signaling pathway (Arite et al., 2009).

Other roles of SLs in regulating plant architectures were recently described, such as their involvement in root growth (Kapulnik et al., 2011; Ruyter-Spira et al., 2011), in the stimulation of cambium activity (Agusti et al., 2011), and in nodule formation in planta (Soto et al., 2010; Foo and Davies, 2011). Whether this SL SAR study for the control of branching applies for these novel hormonal effects will need further investigation.

Comparison with Structural Requirements of SLs for Hyphal Branching in AM Fungi and for Seed Germination of Parasitic Plants

The structural requirements of SLs for hyphal branching in AM fungi (Akiyama et al., 2010) and for seed germination of parasitic plants (Xie et al., 2008; Kim et al., 2010) have been extensively studied, revealing the importance of the stereochemistry at C2′ and the absolute configuration for both functions in contrast to SL requirements for branching inhibition. Various SL mimics were synthesized and tested (Zwanenburg et al., 2009; Zwanenburg and Mwakaboko, 2011) essentially for seed germination of the parasitic plant function, due to the relative easiness and well-known expertise to perform these bioassays.

One main common structural requirement between the three SL functions is the CD-ring moiety. The truncation of the AB-rings and even the ABC-rings (see compound **31**) has no consequence on hormonal activity, whereas GR5 is inactive for hyphal branching and significantly less active for seed germination. The oxygenation of the SL backbone has a significant effect on the germination of parasitic weeds (Kim et al., 2010), contrary to the effect on AM fungi hyphal branching (Akiyama et al., 2010) or on pea branching inhibition.

Because in the putative receptor site, only nucleophilic functionalities would be available for initiating a reaction, two mechanisms involving in each case a Michael addition have been proposed for seed

Table VII. *EC_{50} of SL analogs on P. ramosa*

Compound	EC_{50}	SE
	M	
GR24	2.13×10^{-12}	1.18×10^{-12}
GR5	3.44×10^{-10}	2.19×10^{-10}
23	1.9×10^{-8}	1.7×10^{-9}
30	3.0×10^{-7}	1.1×10^{-8}

germination activity. Initially, Zwanenburg et al. (2009) suggested the initial binding of the SL followed by a nucleophilic attack in a Michael fashion at the enol ether bridge. Due to the activity in this recently found model of 2-aryloxyfuranone (Zwanenburg and Mwakaboko, 2011), Zwanenburg proposed an alternative mechanism. A nucleophile would add to the furanone also in a Michael fashion, followed by elimination of the group at C2 after an internal proton shift. Our results show that the enol function is important for bud outgrowth inhibition. Without this chemical function, the activity of the SL analogs decreases but always exists, as for hyphal branching in AM fungi (Akiyama et al., 2010) and for the parasitic plant model but differing according to the species (Mangnus and Zwanenburg, 1992; this study). The higher activity of **23** and **31** in comparison with other SLs in the pea branching test suggests that the mechanisms proposed by Zwanenburg and Mwakaboko (2011) for seed germination of parasitic plants may be different for branching inhibition: no internal proton shift could be involved with these last structures. Globally, important SL structure variations seem to affect bioactivity dramatically for AM fungi hyphal branching, moderately for parasitic seed germination stimulation, and weakly for the shoot branching inhibition. These observations would suggest that each system uses a distinct perception system. In accordance with our data, an alternative mechanism for the SL mode of action involving the hydrolysis of the butenolide D-ring was very recently proposed (Scaffidi et al., 2012).

This work confirmed the essential role of the D-ring for SL bioactivity for different biological functions. The γ-butyrolactones and specifically α,β-unsaturated furanones, including SLs with their D-ring, are important natural chemical mediators. Indeed, this class of compounds are found as pheromones (Tumlinson et al., 1977), allelochemicals, or *N*-acyl homo-Ser lactones, hormone-like signals by which bacteria can communicate with each other and coordinate their gene expression in a cell density-dependent manner, a process known as quorum sensing (Galloway et al., 2011). SLs represent a fascinating example of plant hormones with multiple signaling roles between different kingdoms, in parasitic interaction between plants, or between moss individuals to regulate their extension and the potential structure of moss communities (Proust et al., 2011). Whether these roles derived from their specific structures is an intriguing question (Tsuchiya and McCourt, 2012). The identification of SL receptors and signaling pathways in the different systems will help us better understand the evolution of functions of this remarkable and intriguing class of compounds.

CONCLUSION

SL structural requirements for shoot branching inhibition were determined through the study of 42 various natural SLs and analogs and are summarized in Figure 14. The presence of the D-ring is essential for hormonal activity. The stereochemistry at C2′ is not an important structural feature for potent activity. The most active SL analogs for bud outgrowth repression were found to be GR5 and analogs **23** and **31** possessing a 3,4-dimethylbutenolide D-ring, and not GR24, which was previously found to be the most active SL analog for inducing arasitic weed germination (Zwanenburg et al., 2009) and for AM fungi hyphal branching (Besserer et al., 2006; Akiyama et al., 2010). These results suggest, to our knowledge for the first time, that branching signal recognition could present some distinctive features, compared with the perception of the signal for the different models. These results established that an SL analog, compound **23** or **31**, could be used to control plant architecture without favoring the parasitic plant *P. ramosa*. We have demonstrated that the presence of both an α,β-unsaturated system and a methylbutenolide or dimethylbutenolide as the D-ring in the same molecule is essential. Our SAR study establishes that SLs show potent activity in a structure-dependent manner via a receptor-mediated mechanism but with low specificity concerning the stereochemistry or the substitution of SLs. Genetic approaches using branching mutants not responding to exogenous SL applications and analogy with other hormone signaling pathways have led to two candidate proteins for the SL receptor, the F-box protein encoded by the *MAX2/RMS4/D3* gene and the D14 protein of the α/β-fold hydrolase superfamily (Arite et al., 2009; Beveridge and Kyozuka, 2010). Once identified, the SL receptor may be used for the development of other assays to investigate ligand specificity.

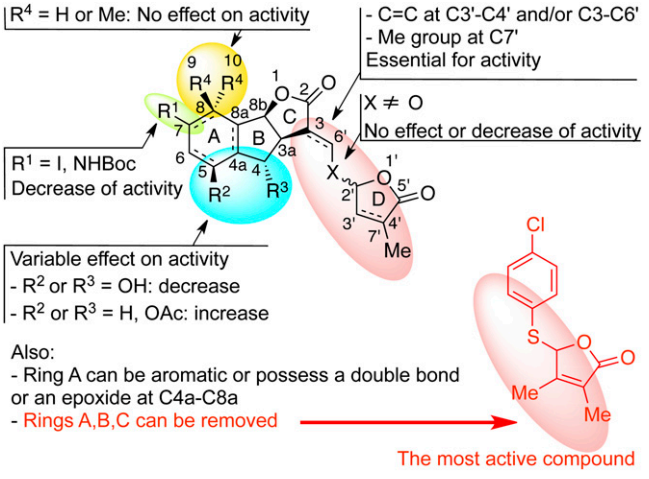

Figure 14. Effects of SL structural modifications on bud outgrowth inhibition in the pea model. Ac, Acetyl; Boc, *t*-butoxycarbonyl; Me, methyl.

MATERIALS AND METHODS

General Remarks

Infrared (IR) spectra were recorded as neat. ^{1}H- and ^{13}C-NMR spectra were recorded as solutions in $CDCl_3$, using residual protic solvent $C\underline{H}Cl_3$ (δ_H = 7.24 ppm) or $\underline{C}DCl_3$ (δ_C = 77.23 ppm) as an internal reference. Mass spectra were determined by electrospray ionization (ESI). All reactions were monitored by thin-layer chromatography carried out on 0.2-mm aluminum silica gel precoated plates using UV light and a 5% ethanolic solution of phosphomolybdic acid and heat as staining agent. Flash chromatography was performed on 40- to 63-μm (400–230 mesh) silica gel 60 with EtOAc-heptane as eluents. Commercially available reagents and solvents were purified and dried when necessary by the usual methods. Tetrahydrofuran (THF) and diethyl ether were purified by distillation, under nitrogen, from sodium/benzophenone. *N*,*N*-Dimethylformamide and CH_2Cl_2 were dried by distillation from calcium hydride and acetone from anhydrous $CaSO_4$. Unless otherwise mentioned, all other reagents were purchased from commercial sources and were used without further purification.

GR24, 2′-epi-GR24, and derivatives **1**, 2′-epi-**1**, **2**, 2′-epi-**2**, **4**, and **5** (Fig. 2) were prepared according to the procedures described (Mangnus et al., 1992; Mangnus and Zwanenburg, 1992; Thuring et al., 1997; Reizelman et al., 2003); compound **3** was prepared according to the procedure described by Fell and Harbridge (1990) and d'orenone according to the procedure of Schachtschabel and Boland (2007). (+)- and (−)-Solanacol and solanacyl acetate were prepared by the procedure described previously in our laboratory (Chen et al., 2010). GR5 was synthesized by known procedures (Johnson et al., 1981), natural SLs (orobanchol, orobanchyl acetate, fabacyl acetate) were generously supplied by Prof. K. Yoneyama, and SLs (strigol, strigyl acetate, 5-deoxystrigol, sorgolactone) were derived by organic synthesis using known procedures or supplied by Bayer CropScience.

(3a*R**,8b*S**,*E*)-3-((Dibenzylamino)methylene)-3,3a,4,8b-tetrahydro-2*H*-indeno[1,2-*b*]furan-2-one 7

Tricycle **6** (Mangnus et al., 1992; 20 mg, 0.099 mmol, 1 eq.), dibenzylamine (20 mg, 0.099 mmol, 1 eq.), and $Fe(OTf)_3 \cdot 6.2DMSO$ (**11**), where Tf = trifluoromethanesulfonyl and DMSO = dimethyl sulfoxide (Antoniotti and Duñach, 2008; 14 mg, 0.015 mmol, 0.15 eq.), were dissolved in anhydrous CH_2Cl_2 (1 mL). The reaction mixture was heated to 60°C under microwave irradiation (300 W) for 2 h. The reaction mixture was cooled and poured into a separation funnel containing CH_2Cl_2 (20 mL) and $NaHCO_3$ (saturated aqueous 20 mL). The combined organic extracts were washed with water (10 mL), dried over Na_2SO_4, and evaporated under reduced pressure. The crude material was purified by chromatography on a silica gel (heptane:EtOAc 9:1 to 1:1) to give the desired product **7** (38 mg, quantitative) as a white solid. ^{1}H-NMR (500 MHz, $CDCl_3$) δ 7.64 (s, 1 H), 7.48 (d, J = 7.3 Hz, 1 H), 7.41 to 7.17 (m, 12 H), 7.15 (d, J = 7.6 Hz, 1 H), 5.72 (d, J = 8.2 Hz, 1 H), 4.54 (d, J = 15.6 Hz, 2 H), 4.32 (d, J = 15.6 Hz, 2 H), 3.87 to 3.80 (m, 1 H), 3.25 (dd, J = 16.2, 9.2 Hz, 1 H), 3.03 (dd, J = 16.2, 4.6 Hz, 1 H). ^{13}C-NMR (75 MHz, $CDCl_3$) δ 175.5 (C), 147.5 (CH), 142.8 (C), 139.9 (C), 136.5 (2 C), 129.9 (CH), 129.3 (4 CH), 128.3 (2 CH), 127.5 (5 CH), 126.7 (CH), 125.1 (CH), 95.1 (C), 84.6 (CH), 55.0 (br s, CH_2), 53.4 (br s, CH_2), 42.6 (CH_2), 40.2 (CH). Mass spectrometry (MS) mass-to-charge ratio (m/z) 382 (MH^+, 100%). High Resolution Mass Spectrometry (ESI) m/z calculated for $C_{26}H_{24}NO_2$ [M + H^+]: 382.1807; found: 382.1797.

(3a*R**,8b*S**,*E and Z*)-3-((Benzylamino)methylene)-3,3a,4,8b-tetrahydro-2*H*-indeno[1,2-*b*]furan-2-one 9

Prepared from tricycle **6** by the same procedure as for **7** to give **9** as a slightly yellow amorphous solid (58 mg, quantitative). Major isomer: ^{1}H-NMR (300 MHz, acetone D_6) δ 7.75 to 7.61 (br s, 1 H, NH), 7.32 to 7.07 (m, 9 H), 6.99 (d, J = 1.3 Hz, 1 H), 5.69 (d, J = 7.9 Hz, 1 H), 5.55 (d, AB, J = 6.2 Hz, 2 H), 3.74 (tt, J = 7.9, 3.2 Hz, 1 H), 3.23 (dd, J = 16.4, 8.1 Hz, 1 H), 3.23 (dd, J = 16.4, 2.1 Hz, 1 H). ^{13}C-NMR (75 MHz, acetone D_6) δ 174.0 (C), 149.4 (CH), 143.7 (C), 141.9 (C), 140.6 (C), 130.1 (CH), 129.5 (2 CH), 128.2 (CH), 128.1 (2 CH), 127.8 (CH), 126.8 (CH), 126.2 (CH), 94.4 (C), 86.0 (CH), 52.6 (CH_2), 41.3 (CH_2), 41.2 (CH). MS (ESI) m/z (%) 605 (50), 346 (25), 314 (100), 292 (30). HRMS (ESI) m/z calculated for $C_{19}H_{17}NO_2Na$ [M + Na^+]: 314.1157; found: 314.1167.

(3a*R**,8b*S**,*Z*)-3-((1,3,4,6-Tetra-*O*-acetyl-2-amino-2-deoxy-α-D-glucopyranosyl)methylene)-3,3a,4,8b-tetrahydro-2*H*-indeno[1,2-*b*]furan-2-one 10

Tricycle **6** (20 mg, 0.099 mmol, 1 eq.), 2-acetamido-1,3,4,6-tri-*O*-acetyl-2-deoxy-β-D-glucopyranoside **8** (116 mg, 0.297 mmol, 3 eq.), and $Fe(OTf)_3 \cdot 6.2DMSO$ (**11**; 43 mg, 0.045 mmol, 0.45 eq.) were dissolved in anhydrous CH_2Cl_2 (1 mL). The reaction mixture was heated to 60°C under microwave irradiation (300 W) for 2 h. The reaction mixture was cooled and poured into a separation funnel containing CH_2Cl_2 (20 mL) and $NaHCO_3$ (sat. aq. 20 mL). The combined organic extracts were washed with water (10 mL), dried over Na_2SO_4, and evaporated under reduced pressure. The crude material was purified by chromatography on a silica gel (heptane:EtOAc 9:1 to 1:1) to give the desired mixture of inseparable diastereoisomers **10** (26 mg, 49%) as an off-white solid. ^{1}H-NMR (500 MHz, $CDCl_3$) δ 7.48 to 7.12 (m, 10H), 6.60 (d, J = 5.8 Hz, 1 H), 6.57 (d, J = 5.8 Hz, 1 H), 6.17 (d, J = 3.7 Hz, 1 H), 6.10 (d, J = 3.7 Hz, 1 H), 5.86 (d, J = 4.5 Hz, 1 H), 5.85 (d, J = 4.5 Hz, 1 H), 5.28 (t, J = 10.1 Hz, 1 H), 5.22 (t, J = 10.1 Hz, 1 H), 5.10 to 5.02 (m, 2 H), 4.31 (t, J = 3.7 Hz, 1 H), 4.28 (t, J = 3.7 Hz, 1 H), 4.06 to 3.98 (m, 4 H), 3.83 to 3.75 (m, 2 H), 3.49-3.42 (m, 2 H), 3.41-3.32 (m, 2 H), 2.85 (d, J = 16.5 Hz, 1 H), 2.77 (d, J = 16.5 Hz, 1 H), 2.20 (s, 3 H), 2.15 (s, 3 H), 2.05 (s, 6 H), 2.01 (s, 6 H), 1.99 (s, 3 H), 1.83 (s, 3 H). ^{13}C-NMR (75 MHz, $CDCl_3$) δ 173.8 (C), 173.7 (C), 170.7 (2 C), 170.0 (C), 169.9 (C), 169.8 (2 C), 169.1 (C), 169.0 (C), 145.6 (CH), 145.5 (CH), 142.3 (C), 142.0 (C), 140.1 (C), 140.0 (C), 129.9 (CH), 129.8 (CH), 127.7 (CH), 127.6 (CH), 126.7 (CH), 126.5 (CH), 125.5 (CH), 125.2 (CH), 97.6 (C), 97.3 (C), 91.1 (CH), 91.0 (CH), 86.2 (CH), 86.1 (CH), 71.7 (CH), 71.5 (CH), 70.0 (CH), 69.9 (CH), 68.1 (2 CH), 61.7 (2 CH_2), 60.2 (CH), 60.0 (CH), 40.5 (2 CH_2), 40.3 (CH), 40.2 (CH), 21.0 (CH_3), 20.9 (3 CH_3), 20.8 (3 CH_3), 20.6 (CH_3). MS m/z 554 (MNa^+, 100%). HRMS (ESI) m/z calculated for $C_{26}H_{29}NNaO_{11}$ [M + Na^+]: 554.1639; found: 554.1633.

(3a*R**,8b*S**,*E*)-3-((((*RS**)-5-Oxo-2,5-dihydrofuran-2-yl)oxy)methylene)-3,3a,4,8b-tetrahydro-2*H*-indeno[1,2-*b*]furan-2-one 19 and 2′-epi-19

Tricycle **6** (90 mg, 0.445 mmol, 1 eq.), 5-bromo-2(5*H*)-furanone **12** (Wolff and Hoffmann, 1988; 109 mg, 0.668 mmol, 1.5 eq.), and anhydrous K_2CO_3 (100 mg, 0.890 mmol, 2 eq.) were dissolved in anhydrous acetone (10.8 mL). The reaction mixture was stirred for 3 h and concentrated under reduced pressure. The residue was dissolved in EtOAc (10 mL), filtered, evaporated under reduced pressure, and purified by chromatography on a silica gel (EtOAc:heptane 2:3 to 4:1) to give the desired products **19** (22 mg, 17%) and 2′-epi-**19** (24 mg, 19%) as white amorphous solids. **19**: ^{1}H-NMR (500 MHz, $CDCl_3$) δ 7.50 to 7.48 (br s, 1 H), 7.46 (d, J = 2.4 Hz, 1 H), 7.37 (dd, J = 5.7, 1.3 Hz, 1 H), 7.35 to 7.20 (m, 3 H), 6.40 (dd, J = 5.7, 1.1 Hz, 1 H), 6.28 (t, J = 1.1 Hz, 1 H), 5.93 (d, J = 7.7 Hz, 1 H), 3.97 to 3.89 (m, 1 H), 3.41 (dd, J = 17.0 and 9.4 Hz, 1 H), 3.07 (dd, J = 17.0 and 3.0 Hz, 1 H). ^{13}C-NMR (75 MHz, $CDCl_3$) δ 171.4 (C), 169.0 (C), 151.2 (CH), 148.7 (CH), 142.8 (C), 139.1 (C), 130.4 (CH), 127.8 (CH), 126.8 (2 CH), 125.3 (CH), 114.0 (C), 102.2 (CH), 86.2 (CH), 39.1 (CH), 35.5 (CH_2). IR ν_{max} (film): 3,104, 2,925, 2,855, 1,793, 1,746, 1,680, 1,610 cm^{-1}. HRMS (ESI) m/z calculated for $C_{16}H_{13}O_5$ [M + H^+]: 285.0763; found: 285.0760. 2′-Epi-**19**: ^{1}H-NMR (500 MHz, $CDCl_3$) δ 7.47 (d, J = 2.4 Hz, 1 H), 7.45 to 7.43 (br s, 1 H), 7.37 (dd, J = 5.7, 1.3 Hz, 1 H), 7.34 to 7.19 (m, 3 H), 6.39 (dd, J = 5.8, 1.3 Hz, 1 H), 6.29 (t, J = 1.1 Hz, 1 H), 5.93 (d, J = 7.9 Hz, 1 H), 3.95 to 3.87 (m, 1 H), 3.39 (dd, J = 17.0, 9.2 Hz, 1 H), 3.06 (dd, J = 17.0, 3.0 Hz, 1 H). ^{13}C-NMR (75 MHz, $CDCl_3$) δ 171.4 (C), 169.0 (C), 151.3 (CH), 148.8 (CH), 142.7 (C), 138.8 (C), 130.3 (CH), 127.7 (CH), 126.53 (CH), 126.50 (CH), 125.4 (CH), 113.9 (C), 102.3 (CH), 86.2 (CH), 39.0 (CH), 37.5 (CH_2). IR ν_{max} (film): 3,102, 2,931, 2,856, 1,793, 1,744, 1,679, 1,610 cm^{-1}. HRMS (ESI) m/z calculated for $C_{16}H_{13}O_5$ [M + H^+]: 285.0763; found: 285.0769.

(3a*R**,8b*S**,*E*)-3-((((*RS**)-3-Bromo-4-methoxy-5-oxo-2,5-dihydrofuran-2-yl)oxy)methylene)-3,3a,4,8b-tetrahydro-2*H*-indeno[1,2-*b*]furan-2-one 20 and 2′-epi-20

Obtained from tricycle **6** and 3,5-dibromo-2-methoxy-2(5*H*)-furanone **13** by the same procedure as for **19** to give the desired products **20**/2′-epi-**20** (1:1, unseparable mixture; 50 mg, 69%) as a colorless oil. **20**/2′-epi-**20** (1:1): ^{1}H-NMR (300 MHz, $CDCl_3$) δ 7.49 to 7.41 (m, 4 H), 7.35 to 7.21 (m, 6 H), 6.03 (d, J = 4 Hz, 2 H), 5.96 (d, J = 7.9 Hz, 2 H), 4.22 (s, 6 H), 4.00 to 3.94 (m, 2 H), 3.46 (dd, J = 17.0, 9.4 Hz, 2 H), 3.14 (ddd, J = 17.0, 11.9, 2.8 Hz, 2 H). ^{13}C-NMR (75 MHz, $CDCl_3$) δ 171.24 (C), 171.21 (C), 162.3 (2 C), 150.2 (CH), 149.6 (CH), 145.8 (2 C), 142.8 (C), 142.7 (C), 138.9 (C), 138.8 (C), 130.26 (CH), 130.24 (CH), 127.70

(CH), 127.68 (CH), 126.63 (CH), 126.59 (CH), 125.40 (CH), 125.35 (CH), 114.8 (C), 114.6 (C), 107.29 (C), 107.26 (C), 99.60 (CH), 99.57 (CH), 86.24 (CH), 86.19 (CH), 59.3 (2 CH_3), 39.1 (CH), 39.0 (CH), 37.6 (CH_2), 37.1 (CH_2). IR ν_{max} (film): 2,952, 2,856, 1,792, 1,744, 1,669, 1,608 cm^{-1}. HRMS (ESI) m/z calculated for $C_{17}H_{13}O_6BrNa$ [M + Na^+]: 414.9793; found: 414.9808.

(3a*R**,8b*S**,*E*)-3-((((*RS**)-4-Methoxy-5-oxo-2,5-dihydrofuran-2-yl)oxy)methylene)-3,3a,4,8b-tetrahydro-2*H*-indeno[1,2-*b*]furan-2-one 21 and 2′-epi-21

A mixture of compound **20*α*/**2′-epi-**20** (1:1; 15 mg, 0.038 mmol, 1 eq.) and zinc (14 mg, 0.206 mmol, 5.4 eq.). AcOH (one drop) in THF (0.8 mL) was sonicated for 2 h under argon and filtered on a silica gel. The silica gel was washed with EtOAc (2 × 5 mL), and the filtrate was evaporated under reduced pressure. The residue was purified by preparative thin-layer chromatography (EtOAc:heptane 1:1) to afford the two diastereoisomers **21/**2′-epi-**21** (1:1; 10 mg, 83%) as a colorless oil. A sample of **21** (2.5 mg) was obtained by repeated PTLC (EtOAc:heptane 1:1). **21**: ^{1}H-NMR (500 MHz, $CDCl_3$) δ 7.52 to 7.49 (m, 2 H), 7.35 (t, J = 7.6 Hz, 1 H), 7.30 (d, J = 7.6 Hz, 1 H), 7.25 (d, J = 7.6 Hz, 1 H), 6.25 to 6.24 (br s, 1 H), 5.99 (d, J = 1.6 Hz, 1 H), 5.97 (d, J = 7.9 Hz, 1 H) 3.98 to 3.91 (m, 1 H), 3.92 (s, 3 H), 3.04 (dd, J = 17.0, 9.5 Hz, 1 H), 3.12 (dd, J = 17.0, 2.8 Hz, 1 H). ^{13}C-NMR (125 MHz, $CDCl_3$) δ 171.4 (C), 164.0 (C), 151.3 (C), 150.8 (CH), 142.7 (C), 138.9 (C), 130.3 (CH), 127.7 (C), 126.6 (CH), 125.4 (CH), 113.8 (C), 109.3 (CH), 99.8 (CH), 86.1 (CH), 59.1 (CH_3), 39.0 (CH), 37.6 (CH_2). IR ν_{max} (film): 2,937, 2,854, 1,799, 1,747, 1,681, 1,663 cm^{-1}. HRMS (ESI) m/z calculated for $C_{17}H_{14}O_6Na$ [M + Na^+]: 337.0688; found: 337.0704.

(3a*R**,8b*S**,*E*)-3-((((*RS**)-3-Methoxy-5-oxo-2,5-dihydrofuran-2-yl)oxy)methylene)-3,3a,4,8b-tetrahydro-2*H*-indeno[1,2-*b*]furan-2-one 22 and 2′-epi-22

Prepared from tricycle **6** and 5-bromo-4-methoxy-2(5*H*)-furanone **14** (Wolff and Hoffmann, 1988) by the same procedure as for **19** to give the desired products **22/**2′-epi-**22** (1:1, unseparable mixture; 38 mg, 66%) as a colorless oil. **22/**2′-epi-**22** (1:1): ^{1}H-NMR (300 MHz, $CDCl_3$) δ 7.42 (d, J = 7.2 Hz, 2 H), 7.36 (t, J = 2.6 Hz, 2 H), 7.29 to 7.15 (m, 6 H), 5.94 (s, 2 H), 5.88 (d, J = 7.9 Hz, 2 H), 5.22 (d, J = 1.9 Hz, 2 H), 3.92 (s, 3 H), 3.90 (s, 3 H), 3.89 to 3.85 (m, 2 H), 3.38 (dd, J = 17.0, 9.4 Hz, 2 H), 3.05 (dd, J = 17.0, 3.0 Hz, 2 H). ^{13}C-NMR (75 MHz, $CDCl_3$) δ 175.25 (C), 175.23 (C), 171.34 (C), 171.31 (C), 168.46 (C), 168.42 (C), 150.6 (2 CH), 142.84 (C), 142.81 (C), 139.0 (C), 138.9 (C), 130.18 (CH), 130.17 (CH), 127.62 (CH), 127.59 (CH), 126.7 (CH), 126.5 (CH), 125.40 (CH), 125.3 (CH), 114.0 (C), 113.9 (C), 98.3 (CH), 98.1 (CH), 91.5 (CH), 91.4 (CH), 86.12 (CH), 86.10 (CH), 60.41 (CH_3), 60.38 (CH_3), 39.00 (CH), 38.96 (CH), 37.5 (CH_2), 37.4 (CH_2). IR ν_{max} (film): 3,124, 3,029, 2,946, 2,858, 1,792, 1,745, 1,680, 1,646 cm^{-1}. HRMS (ESI) m/z calculated for $C_{17}H_{14}O_6Na$ [M + Na^+]: 337.0688; found: 337.0701.

(3a*R**,8b*S**,*E*)-3-((((*RS**)-3,4-Dimethyl-5-oxo-2,5-dihydrofuran-2-yl)oxy)methylene)-3,3a,4,8b-tetrahydro-2*H*-indeno[1,2-*b*]furan-2-one 23 and 2′-epi-23

Prepared from tricycle **6** and 5-chloro-3,4-dimethyl-2(5*H*)-furanone **15** (Canevet and Graff, 1978) by the same procedure as for **19** to give the desired products **23/**2′-epi-**23** (1:1; 85 mg, 84%) as a colorless oil. The pure isomer **23** (colorless oil) could be obtained by separation by PTLC (EtOAc:heptane 3:7). **23**: ^{1}H-NMR (300 MHz, $CDCl_3$) δ 7.49 (d, J = 7.2 Hz, 1 H), 7.44 (d, J = 2.6 Hz, 1 H), 7.35 to 7.20 (m, 3 H), 5.90 (s, 1 H), 5.89 (d, J = 7.9 Hz, 1 H), 3.93 to 3.85 (m, 1 H), 3.38 (dd, J = 17.0, 9.4 Hz, 1 H), 3.04 (dd, J = 17.0, 3.4 Hz, 1 H), 2.00 to 1.98 (m, 3 H), 1.86 to 1.84 (m, 3 H). ^{13}C-NMR (75 MHz, $CDCl_3$) δ 171.4 (C), 170.8 (C), 152.3 (C), 151.2 (CH), 142.7 (C), 139.1 (C), 130.2 (CH), 128.8 (C), 127.7 (CH), 126.7 (CH), 125.3 (CH), 113.1 (C), 102.5 (CH), 86.1 (CH), 39.1 (CH), 37.6 (CH_2), 11.6 (CH_3), 8.9 (CH_3). IR ν_{max} (film): 3,056, 2,927, 2,857, 1,775, 1,744, 1,677, 1,608 cm^{-1}. HRMS (ESI) m/z calculated for $C_{18}H_{16}O_5Na$ [M + Na^+]: 335.0895; found: 335.0899.

(3a*R**,8b*S**,*E*)-3-(((-(*RS**)-2,3,4-Trimethyl-5-oxo-2,5-dihydrofuran-2-yl)oxy)methylene)-3,3a,4,8b-tetrahydro-2*H*-indeno[1,2-*b*]furan-2-one 25 and 2′-epi-25

Prepared from tricycle **6** and 5-chloro-2,3,4-trimethyl-2(5*H*)-furanone **17** by the same procedure as for **19** to give the desired products **25/**2′-epi-**25** (48.7 mg, 78%; mixture of diastereoisomers, 1:1) as a white amorphous solid. The furanone **17** was prepared from 5-hydroxy-2,3,4-dimethyl-2(5*H*)-furanone (Surmont et al., 2010) by the procedure of Canevet and Graff (1978). **25/**2′-epi-**25**: ^{1}H-NMR (300 MHz, $CDCl_3$) δ 7.42 (d, J = 7.3 Hz, 2 H), 7.30 to 7.17 (m, 6 H), 7.09 (d, J = 2.6 Hz, 2 H), 5.88 (d, J = 7.9 Hz, 2 H), 3.90 to 3.83 (m, 2 H), 3.40 (dd, J = 17.0, 9.2 Hz, 2 H), 3.09 (dd, J = 17.0, 3.2 Hz, 2 H), 1.90 (d, J = 1.1 Hz, 6 H), 1.83 (d, J = 1.1 Hz, 6 H), 1.70 (s, 6 H). ^{13}C-NMR (75 MHz, $CDCl_3$) δ 171.6 (2 C), 170.9 (2 C), 155.7 (C), 155.6 (C), 147.6 (CH), 147.5 (CH), 142.8 (C), 142.7 (C), 139.07 (C), 138.98 (C), 130.1 (2 CH), 127.7 (CH), 127.6 (CH), 128.0 (C), 127.95 (C), 126.6 (CH), 126.5 (CH), 125.4 (CH), 125.2 (CH), 113.4 (C), 113.3 (C), 107.8 (C), 107.7 (C), 85.99 (CH), 85.97 (CH), 39.06 (CH), 38.98 (CH), 37.6 (CH_2), 37.5 (CH_2), 22.69 (CH_3), 22.62 (CH_3), 10.7 (2 CH_3), 8.9 (2 CH_3). IR ν_{max} (film): 2,928, 1,777, 1,746, 1,673 cm^{-1}. HRMS (ESI) m/z calculated for $C_{19}H_{19}O_5$ [M + H^+]: 327.1232; found: 327.1224.

(3a*R**,8b*S**,*E*)-3-(((-(*RS**)-*3*-Butyl-4-methyl-5-oxo-2,5-dihydrofuran-2-yl)oxy)methylene)-3,3a,4,8b-tetrahydro-2*H*-indeno[1,2-*b*]furan-2-one 26 and 2′-epi-26

Prepared from tricycle **6** and 5-chloro-3-butyl-4-methyl-2(5*H*)-furanone **18** by the same procedure as for **19** to give the desired products **26/**2′-epi-**26** (80.2 mg, 91%; mixture of diastereoisomers, 1:1) as a white amorphous solid. The furanone **18** was prepared from 5-hydroxy-3-butyl-4-methyl-2(5*H*)-furanone (Schreiber and Wermuth, 1965) by the procedure of Canevet and Graff (1978). ^{1}H-NMR (300 MHz, $CDCl_3$) δ 7.48 to 7.43 (m, 4 H), 7.35 to 7.19 (m, 6 H), 6.03 (br s, 2 H), 5.93 (d, J = 7.7 Hz, 2 H), 3.96 to 3.87 (m, 2 H), 3.40 (dt, J = 17.3, 8.9 Hz, 2 H), 3.40 (dt, J = 17.3, 3.6 Hz, 2 H), 2.52 to 2.30 (m, 4 H), 1.89 (s, 6 H), 1.42 to 1.31 (m, 8 H), 0.94 (q, J = 7.2 Hz, 6 H). ^{13}C-NMR (75 MHz, $CDCl_3$) δ 171.41 (C), 171.37 (C), 171.02 (C), 170.98 (C), 156.43 (C), 156.28 (C), 151.4 (CH), 151.3 (CH), 142.7 (C), 142.6 (C), 139.0 (C), 138.9 (C), 130.2 (2 CH), 128.5 (C), 128.4 (C), 127.7 (CH), 127.6 (CH), 126.6 (CH), 126.5 (CH), 125.4 (CH), 125.2 (CH), 113.4 (C), 113.2 (C), 101.85 (CH), 101.82 (CH), 86.04 (CH), 86.02 (CH), 39.0 (2 CH), 37.63 (CH_2), 37.56 (CH_2), 29.46 (CH_2), 29.43 (CH_2), 26.03 (CH_2), 25.98 (CH_2), 22.89 (CH_2), 22.81 (CH_2), 13.9 (2 CH_3), 8.9 (2 CH_3). IR ν_{max} (film): 2,930, 1,778, 1,749, 1,681 cm^{-1}. HRMS (ESI) m/z calculated for $C_{21}H_{23}O_5$ [M + H^+]: 355.1545; found: 355.1535.

(*E*)-((3a*R**,8b*S**)-2-Oxo-3a,4-dihydro-2*H*-indeno[1,2-*b*]furan-3(8b*H*)-ylidene)methylbenzoate 27

Prepared from tricycle **6** and 3-bromo-2-benzoyloxy-2(5*H*)-furanone **16** by the same procedure as for **19** to give the compound **27** (20 mg, 26%) as a white solid. Furanone **16** was obtained by bromation of 2-benzoyloxy-2-buten-4-olide (Limberg and Thiem, 1995) by the same procedure as for 5-bromo-3-methyl-2(5*H*)-furanone (Macalpine et al., 1976). Melting point, 164.2°C to 165.3°C (heptane:EtOAc). ^{1}H-NMR (300 MHz, $CDCl_3$) δ 8.46 (d, J = 2.6 Hz, 1 H), 8.09 (d, J = 7.2 Hz, 1 H), 8.07 (d, J = 1.2 Hz, 1 H), 7.63 (dt, J = 7.3, 1.3 Hz, 1 H), 7.51 to 7.45 (m, 3 H), 7.31 to 7.17 (m, 3 H), 5.97 (d, J = 7.9 Hz, 1 H), 4.14 to 4.06 (m, 1 H), 3.59 (dd, J = 16.8, 9.4 Hz, 1 H), 3.21 (dd, J = 16.8, 3.4 Hz, 1 H). ^{13}C-NMR (75 MHz, $CDCl_3$) δ 171.0 (C), 162.1 (C), 143.9 (CH), 142.5 (C), 138.9 (C), 134.9 (CH), 130.5 (2 CH), 130.4 (CH), 129.2 (2 CH), 127.9 (CH), 127.8 (C), 126.7 (CH), 125.4 (CH), 116.7 (C), 86.1 (CH), 39.4 (CH), 37.8 (CH_2). IR ν_{max} (film): 3,076, 2,929, 2,855, 1,756, 1,684, 1,600 cm^{-1}. HRMS (ESI) m/z calculated for $C_{19}H_{15}O_4$ [M + H^+]: 307.0970; found: 307.0971.

(*E*)-5,5′-(((2-Oxodihydrofuran-3(2*H*)-ylidene)methyl)azanediyl)bis(3,4-dimethylfuran-2(5*H*)-one) 29

To a −10°C solution of 3-aminomethylenedihydrofuran-2-one **28** (Zanatta et al., 2003; 100 mg, 0.876 mmol, 1 eq.) in THF (5 mL) was added NaH (67 mg, 60% weight in mineral oil, 1.665 mmol, 1.9 eq.), and the resulting solution was stirred under argon for 30 min at this temperature and then cooled to −78°C, and the chlorobutenolide **15** (321 mg, 2.191 mmol, 2.5 eq.) was added to the reaction mixture. The solution was warmed to room temperature, stirred for 2.5 h, quenched with AcOH (0.5 mL) followed by water, and extracted with EtOAc (3 × 10 mL). The combined organic layers were washed with brine (10 mL), dried ($MgSO_4$), filtered, and evaporated under reduced pressure. The residue was purified by chromatography on a silica gel (EtOAc:heptane 1:1) to give 22 mg of the compound **29** (8%) as an amorphous solid. ^{1}H-NMR (500 MHz, $CDCl_3$) δ 7.87 (t, J = 2.4 Hz, 1 H), 5.83 (s, 1 H), 5.29 (s, 1 H), 4.43 to 4.25 (m, 2 H), 3.40 to 3.29 (m, 1 H), 3.40 to 3.29 (m, 1 H), 2.11 (s, 3 H), 1.89 (t, J = 1.0 Hz, 3 H), 1.78 (s, 6 H). ^{13}C-NMR (125 MHz, $CDCl_3$) δ 172.8 (C), 171.8 (C), 169.4

(C), 153.4 (C), 150. 8 (C), 131.8 (C), 128.0 (CH), 127.5 (C), 105.0 (C), 95.1 (CH), 86.7 (CH), 65.2 (CH_2), 25.8 (CH_2), 12.9 (CH_3), 11.5 (CH_3), 8.8 (CH_3), 8.7 (CH_3). IR ν_{max} (film): 2,923, 1,748, 1,659, 1,589 cm^{-1}. HRMS (ESI) m/z calculated for $C_{17}H_{20}NO_6$ [M + H^+]: 334.1278; found: 334.1291.

(*E*)-3,4-Dimethyl-5-((2-oxodihydrofuran-3(2*H*)-ylidene) methoxy)furan-2(5*H*)-one 30

Potassium *tert*-butoxide (469 mg, 0.418 mmol, 1.2 eq.) was added to a mixture of γ-butyrolactone (300 mg, 0.28 mL, 3.48 mmol, 1 eq.) and ethyl formate (0.34 mL, 4.18 mmol, 1.2 eq.) in THF (7.5 mL) at 0°C under argon and stirred for 2 h. It was then cooled to −78°C, and the chlorobutenolide **15** (562 mg, 3.83 mmol, 1.3 eq.) was gradually added. The mixture was then warmed to room temperature and stirred for 18 h. The reaction mixture was evaporated under reduced pressure, diluted with CH_2Cl_2 (10 mL), and the organic layer was washed with an aqueous solution of acetic acid (5%, 10 mL). The aqueous phase was extracted with CH_2Cl_2 (2 × 10 mL), and the combined organic layers were evaporated under reduced pressure. The crude product was purified by chromatography on a silica gel (heptane:EtOAc 3:2 to 1:1) to afford **30** (292 mg, 37%) as a white solid. Melting point, 93.4°C to 93.8°C (heptane:EtOAc). ^{1}H-NMR (300 MHz, $CDCl_3$) δ 7.42 (t, *J* = 2.8 Hz, 1 H), 5.93 (s, 1 H), 4.35 (t, *J* = 7.5 Hz, 2 H), 2.88 (td, *J* = 7.5, 2.8 Hz, 2 H), 1.99 (t, *J* = 1.0 Hz, 3 H), 1.87 (t, *J* = 1.0 Hz, 3 H). ^{13}C-NMR (75 MHz, $CDCl_3$) δ 171.9 (C), 170.9 (C), 152.5 (C), 150.0 (CH), 128.5 (C), 107.6 (CH), 102.3 (CH), 66.0 (CH_2), 24.1 (CH_2), 11.6 (CH_2), 8.8 (CH_2). IR ν_{max} (film): 2,987, 2,923, 1,771, 1,748, 1,685 cm^{-1}. HRMS (ESI) m/z calculated for $C_{11}H_{13}O_5$ [M + H^+]: 225.0763; found: 225.0755.

5-((4-Chlorophenyl)thio)-3,4-dimethylfuran-2(5*H*)-one 31

Prepared from 4-chlorobenzenethiol and 5-chloro-3,4-dimethyl-2(5*H*)-furanone **15** (Canevet and Graff, 1978) by the same procedure as for **19** to give the desired product **31** (361 mg, 51%) as a white solid. Melting point, 74.5°C to 76.9°C. ^{1}H-NMR (300 MHz, $CDCl_3$) δ 7.34 (dt, *J* = 8.7, 2.1 Hz, 2 H), 7.20 (dt, *J* = 8.7, 2.1 Hz, 2 H), 5.83 to 5.82 (m, 1 H), 1.96 (t, *J* = 1.0, 3 H), 1.64 (t, *J* = 1.0, 3 H). ^{13}C-NMR (75 MHz, $CDCl_3$) δ 172.6 (C), 155.2 (C), 135.4 (C), 135.2 (2 CH), 129.2 (2 CH), 128.2 (C), 126.2 (C), 88.1 (CH), 12.6 (CH_3), 8.5 (CH_3). IR ν_{max} (film): 2,924, 1,758, 1,673, 1,476, 1,093, 985 cm^{-1}. HRMS (ESI) m/z calculated for $C_{12}H_{12}ClO_2S$ [M + H]$^+$: 255.0247; found: 255.0245.

(3a*R**,8b*S**,*E*)-3-(((*R***S**)-4-Methyl-5-oxo-2,5-dihydrofuran-2-yl)thio)methylene)-3,3a,4,8b-tetrahydro-2*H*-indeno[1,2-*b*] furan-2-one 33

To a solution of tricycle **6** (100 mg, 0.495 mmol, 1 eq.) in dry *N*,*N*-dimethylformamide (2 mL) was added MeI (0.111 mL, 1.978 mmol, 4 eq.) and dry K_2CO_3 (89 mg, 0.643 mmol, 1.3 eq.). The reaction mixture was stirred for 3 h at room temperature and diluted with *t*-butylmethylether (20 mL), and the resulting mixture was washed with water (3 × 20 mL). The organic phase was separated, dried ($MgSO_4$), filtered, and evaporated under reduced pressure. The residue was purified by chromatography on a silica gel (EtOAc:heptane 3:7) to give 68 mg of the ether intermediate (53%) as a white solid. To a solution of ether intermediate (19 mg, 0.087 mg, 1 eq.) in a mixture of methanol (0.4 mL) and dioxane (1 mL) was added at room temperature NaHS (10 mg, 0.87 mmol, 10 eq.). The reaction mixture was warmed to 70°C for 3 h, cooled to room temperature, and evaporated under reduced pressure. Acetone (2 mL) was added to the residue, followed by 5-bromo-3-methyl-2(5*H*)-furanone **32** (35 mg, 0.2 mmol, 2.3 eq.) and dry K_2CO_3 (26 mg, 0.19 mmol, 2.2 eq.). The resulting mixture was stirred for 3 h at room temperature and evaporated under reduced pressure. The residue was purified by chromatography on a silica gel (EtOAc:heptane 3:7 to 1:1) to give 8 mg of the thio compound **33** (29%) as a colorless oil (inseparable mixture of two diastereomers, 1:1). **33** (two diastereoisomers 1:1): ^{1}H-NMR (500 MHz, $CDCl_3$) δ 7.50 (d, *J* = 7.6 Hz, 2 H), 7.47 (d, *J* = 2.5 Hz, 1 H), 7.46 (d, *J* = 2.5 Hz, 1 H), 7.33 (t, *J* = 7.3 Hz, 2 H), 7.27 (t, *J* = 7.3 Hz, 2 H), 7.22 (t, *J* = 7.3 Hz, 2 H), 7.05 to 7.04 (m, 2 H), 6.19 (dt, *J* = 8.2, 1.6 Hz, 2 H), 5.96 (d, *J* = 7.9 Hz, 2 H), 3.84 to 3.79 (m, 2 H), 3.44 (dd, *J* = 16.7, 3.2 Hz, 1 H), 3.42 (dd, *J* = 16.7, 3.2 Hz, 1 H), 3.10 (dd, *J* = 16.7, 4.1 Hz, 1 H), 3.09 (dd, *J* = 16.7, 4.1 Hz, 1 H), 2.02 (s, 6 H). ^{13}C-NMR (125 MHz, $CDCl_3$) δ 171.82 (C), 171.79 (C), 168.5 (2 C), 143.6 (2 CH), 142.58 (C), 142.56 (C), 138.74 (C), 138.70 (C), 134.1 (2 C), 133.7 (CH), 133.4 (CH), 130.4 (2 CH), 129.9 (2 C), 127.9 (2 CH), 126.73 (CH), 126.70 (CH), 125.38 (CH), 125.36 (CH), 85.9 (2 CH), 83.3 (CH), 83.1 (CH), 40.9 (2 CH), 36.7 (2 CH_2), 11.0 (2 CH_3). IR ν_{max} (film): 3,083, 3,030, 2,928, 2,853, 1,767, 1,740, 1,655, 1,621 cm^{-1}. HRMS (ESI) m/z calculated for $C_{17}H_{15}O_4S$ [M + H^+]: 315.0691; found: 315.0681.

(*R**)-2-(2,3-Dihydro-1*H*-inden-2-yl)-3-((2*S**,4*S**)-4-methyl-5-oxotetrahydrofuran-2-yloxy)propanoic acid 34

To a solution of 2′-epi-GR24 (30 mg, 0.101 mmol, 1 eq.) in EtOAc (5 mL) was added the catalyst 10% palladium on carbon (16 mg). The flask was flushed with H_2, and a positive pressure of H_2 was maintained. The mixture was stirred at room temperature under 1 atmosphere of H_2 for 2 h. Then the mixture was filtered through a layer of Celite, and the solvent was removed under reduced pressure. The residue was purified by chromatography on a silica gel (EtOAc) to give 29.3 mg of the lactone **34** (95%) as a colorless oil. ^{1}H-NMR (300 MHz, acetone d_6) δ 7.21 to 7.16 (m, 2 H), 7.13 to 7.08 (m, 2 H), 5.56 (dd, *J* = 5.5, 4.5 Hz, 1 H), 4.05 (dd, *J* = 9.6, 4.5 Hz, 1 H), 3.90 (dd, *J* = 9.6, 8.7 Hz, 1 H), 3.10 to 2.98 (m, 2 H), 2.86 to 2.61 (m, 6 H), 1.76 to 1.65 (m, 1 H), 1.24 (d, *J* = 7.2 Hz, 3 H). ^{13}C-NMR (75 MHz, acetone d_6) δ 178.6 (C), 174.8 (C), 143.43 (C), 143.40 (C), 127.18 (CH), 127.16 (CH), 125.1 (2 CH), 104.3 (CH), 71.2 (CH_2), 40.5 (CH), 37.9 (CH_2), 37.8 (CH_2), 37.1 (CH_2), 35.0 (CH), 16.8 (CH_3). IR ν_{max} (film): 3,200 to 2,480 (br), 2,938, 2,845, 1,775, 1,738, 1,706, 1,146 cm^{-1}. MS (ESI) m/z (%) 327 (100). HRMS (ESI) m/z calculated for $C_{17}H_{20}O_5Na$ [M + Na^+]: 327.1208; found: 327.1222.

(3a*R**,8b*S**,*E*)-3-(((2*S**,4*S**)-4-Methyl-5-oxotetrahydrofuran-2-yloxy)methylene)-3,3a,4,8b-tetrahydro-2*H*-indeno[1,2-*b*] furan-2-one 35

To a solution of 2′-epi-GR24 (25 mg, 0.084 mmol, 1 eq.) in EtOAc (12 mL) was added the catalyst 10% palladium on carbon (2.3 mg). The flask was flushed with H_2, and a positive pressure of H_2 was maintained. The mixture was stirred at room temperature under 1 atmosphere of H_2 for 20 min. Then the mixture was filtered through a layer of Celite, and the solvent was removed under reduced pressure. The residue was purified by chromatography on silica gel (EtOAc: heptane 1:1) to give 13.6 mg of the lactone **35** (54%) as a colorless oil. ^{1}H-NMR (500 MHz, $CDCl_3$) δ 7.48 (d, *J* = 7.2 Hz, 1 H), 7.45 (d, *J* = 2.6 Hz, 1 H), 7.32 (td, *J* = 7.2, 2.5 Hz, 1 H), 7.27 (d, *J* = 7.2 Hz, 1 H), 7.23 (d, *J* = 7.2 Hz, 1 H), 5.93 (d, *J* = 7.9 Hz, 1 H), 5.84 (dd, *J* = 5.7, 3.0 Hz, 1 H), 3.95 to 3.88 (m, 1 H), 3.41 (dd, *J* = 19.0, 9.4 Hz, 1 H), 3.08 (dd, *J* = 19.0, 3.4 Hz, 1 H), 2.84 to 2.71 (m, 2 H), 2.08 (dd, *J* = 8.5, 3.2 Hz, 1 H), 1.43 (d, *J* = 7.0 Hz, 3 H). ^{13}C-NMR (125 MHz, $CDCl_3$) δ 177.4 (C), 171.6 (C), 152.2 (CH), 142.7 (C), 138.9 (C), 130.3 (CH), 127.7 (CH), 126.6 (CH), 125.5 (CH), 113.1 (C), 103.2 (CH), 86.1 (CH), 38.9 (CH), 37.7 (CH_2), 36.0 (CH_2), 33.8 (CH), 17.2 (CH_3). IR ν_{max} (film): 2,936, 2,878, 1,788, 1,746, 1,709, 1,680, 1,592 cm^{-1}. MS (ESI) m/z (%) 623 (40), 355 (20), 323 (100). HRMS (ESI) m/z calculated for $C_{17}H_{16}O_5Na$ [M + Na^+]: 323.0895; found: 323.0897.

(2′*R**,3a*S**,8b*S**)-3′-((*S**)-4-Methyl-5-oxo-2,5-dihydrofuran-2-yloxy)-3a,4-dihydrospiro[indeno[1,2-*b*]furan-3,2′-oxiran]-2(8b*H*)-one 36

To a solution of 2′-epi-GR24 (11 mg, 0.0369 mmol, 1 eq.) in CH_2Cl_2 (1 mL) was added in a solution of freshly distilled dimethyldioxirane (Adam et al., 1991) acetone (2.1 mL, approximately 0.1 M) and stirred at 5°C for 12 h. The solution was allowed to reach room temperature, and the volatiles were evaporated under reduced pressure to give 11.5 mg (quantitative) of the lactone **36** (two diastereoisomers 7:3) as a white solid. ^{1}H-NMR (500 MHz, $CDCl_3$) δ 7.51 (t, *J* = 7.0 Hz, 1 H), 7.40 to 7.27 (m, 3 H), 6.96 to 6.93 (m, 0.3 H), 6.90 to 6.87 (m, 0.7 H), 6.16 to 6.13 (m, 1 H), 6.09 (d, *J* = 6.6 Hz, 0.7 H), 6.05 (d, *J* = 7.5 Hz, 0.3 H), 5.39 (s, 0.7 H), 5.13 (s, 0.3 H), 3.47-3.18 (m, 3 H), 2.00 (s, 3 H). ^{13}C-NMR (125 MHz, $CDCl_3$) δ 171.7 (2 C), 170.8 (2 C), 143.6 (C), 143.2 (C), 142.2 (CH), 141.8 (CH), 138.2 (C), 137.4 (C), 135.8 (C), 135.4 (C), 131.0 (CH), 130.8 (CH), 127.9 (2 CH), 126.7 (CH), 126.6 (CH), 125.6 (CH), 125.3 (CH), 99.4 (CH), 99.1 (CH), 87.1 (CH), 86.5 (CH), 81.6 (CH), 79.9 (CH), 63.6 (C), 61.8 (C), 40.2 (CH), 35.6 (CH), 34.0 (CH_2), 33.3 (CH_2), 11.0 (CH_3), 10.9 (CH_3). IR ν_{max} (film): 2,923, 2,854, 1,769, 1,665, 1,609 cm^{-1}. MS (ESI) m/z (%) 378 (100), 337 (40). HRMS (ESI) m/z calculated for $C_{17}H_{14}O_6Na$ [M + Na^+]: 337.0688; found: 337.0674.

(3*R**,3a*S**,8b*S**)-3-Hydroxy-3-(methoxy((*S**)-4-methyl-5-oxo-2,5-dihydrofuran-2-yloxy)methyl)-3,3a,4,8b-tetrahydro-2*H*-indeno[1,2-*b*]furan-2-one 37

To a solution of epoxide **36** (11 mg, 0.035 mmol, 1 eq.) in a mixture CH_2Cl_2: methanol (1 mL; 1:4) was added *p*-toluenesulfonic acid (1 mg). The mixture

was stirred at room temperature for 4 h and overnight at −20°C. Then the solvents were removed under reduced pressure, and the residue was purified by chromatography on silica gel (EtOAc:heptane 1:1) to give 10.2 mg of the alcohol **37** (two isomers, 7:3; 84%) as a colorless oil. ^{1}H-NMR (500 MHz, $CDCl_3$) δ 7.54 to 7.21 (m, 4 H), 6.96 to 6.94 (m, 0.7 H), 6.93 to 6.91 (m, 0.3 H), 6.20 (t, J = 1.3 Hz, 0.7 H), 6.11 (t, J = 1.3 Hz, 0.3 H), 5.90 (d, J = 5.3 Hz, 0.7 H), 5.68 (d, J = 7.2 Hz, 0.3 H), 4.93 (s, 0.3 H), 4.89 (s, 0.7 H), 3.64 (s, 0.9 H), 3.57 (s, 2.1 H), 3.47 to 3.18 (m, 3 H), 1.97 (t, J = 1.3 Hz, 0.9 H), 1.95 (t, J = 2.1 Hz, 3 H). ^{13}C-NMR (125 MHz, $CDCl_3$) major isomer δ 175.0 (2 C), 144.2 (C), 143.4 (CH), 137.7 (C), 134.0 (C), 130.8 (CH), 127.7 (CH), 126.7 (CH), 125.2 (CH), 105.0 (CH), 101.1 (CH), 86.7 (CH), 79.9 (C), 57.1 (CH_3), 48.9 (CH), 31.1 (CH_2), 10.70 (CH_3). MS (ESI) m/z (%) 378 (100), 337 (40). HRMS (ESI) m/z calculated for $C_{18}H_{18}O_7Na$ [M + Na$^+$]: 369.0950; found: 369.0955.

(3a*R**,8b*S**)-3-((((2*S**,4*S**)-4-Methyl-5-oxotetrahydrofuran-2-yl)oxy)methyl)-3,3a,4,8b-tetrahydro-2*H*-indeno[1,2-*b*]furan-2-one 38

Prepared from compound **5** (Mangnus and Zwanenburg, 1992) by the same procedure as for **35** to give the desired product **38** (5 mg, 50%) as a colorless oil. ^{1}H-NMR (500 MHz, $CDCl_3$) δ 7.46 (d, J = 7.3 Hz, 1 H), 7.33 (t, J = 7.3 Hz, 1 H), 7.29 (d, J = 7.3, 1 H), 7.25 (d, J = 7.3 Hz, 1 H), 5.89 (d, J = 7.3 Hz, 1 H), 5.50 (t, J = 5.7 Hz, 1 H), 4.11 (dd, J = 9.5, 6.9 Hz, 1 H), 3.94 (dd, J = 9.5, 4.1 Hz, 1 H), 3.31 to 3.24 (m, 2 H), 3.12 (d, J = 14.2 Hz, 1 H), 2.68 to 2.56 (m, 3 H), 1.86 to 1.83 (m, 1 H), 1.35 (d, J = 6.9 Hz, 3 H). ^{13}C-NMR (125 MHz, $CDCl_3$) δ 178.5 (C), 176.2 (C), 141.8 (C), 139.0 (C), 130.1 (CH), 127.9 (CH), 126.4 (CH), 125.7 (CH), 103.1 (CH), 86.1 (CH), 69.1 (CH_2), 47.6 (CH), 42.3 (CH_2), 37.1 (CH), 36.6 (CH), 34.5 (CH_2), 17.0 (CH_3). IR ν_{max} (film): 2,925, 2,853, 1,771, 1,608 cm^{-1}. HRMS (ESI) m/z calculated for $C_{17}H_{18}O_5Na$ [M + Na$^+$]: 325.1052; found: 325.1068.

Chemical Stability

Solanacol, solanacyl acetate, GR24, and **23** were tested for their chemical stability in an aqueous solution. Aqueous solutions of the compound to be tested (50 μg mL^{-1}) were incubated at 21°C in the HPLC vials. The compounds were first dissolved in acetone (1 mL). Then, 50 μL of the previous solutions was diluted to the final concentration with ethanol (175 μL) and water (750 μL). Indanol (25 μL of a 1 mg mL^{-1} solution in acetone) as an internal standard was added to each solution. The time course of degradation was monitored by ultra-performance liquid chromatography analysis using an Acquity UPLC HSS C_{18} column (1.8 μm, 2.1 × 50 mm) eluted first by 5% acetonitrile in water containing 0.1% formic acid for 0.5 min, then by a gradient from 5% to 100% acetonitrile in water containing 0.1% formic acid within 6.5 min, and by 100% acetonitrile containing 0.1% formic acid for 3 min. The column was operated at 40°C with a flow rate of 0.6 mL min^{-1}. Compounds eluted from the column were detected with a photodiode array detector. The relative quantity of remaining (no degraded) product was determined by integration comparison with the internal standard.

Plant Assays

Bud Outgrowth Inhibition Activity Assay

Pea (*Pisum sativum*) *rms1* mutant plants (allele *rms1-10* identified in the dwarf line Térèse; Beveridge et al., 1997; Rameau et al., 1997; Sorefan et al., 2003; Gomez-Roldan et al., 2008) deficient in SLs were used for the bioassay. The compound to be tested was applied directly to the bud with a micropipette as 10 μL of solution containing 0.1% acetone with 2% polyethylene glycol 1450, 50% ethanol, and 0.4% dimethyl sulfoxide. Twenty-four plants were sown per treatment in trays (two repetitions of 12 plants). The treatment was generally done 10 d after sowing on the axillary bud at node 4 (or 3). The branches at nodes 1 to 2 were removed to encourage the outgrowth of axillary buds at the nodes above. Nodes were numbered acropetally from the first scale leaf as node 1 and the cotyledonary node as node 0. Bud growth at node 4 (node 3 and node 5 in one bioassay) was measured 8 to 10 d after treatment with digital calipers. Generally, if poor activity or no activity was found at 1 μM concentration, no replication was done. Because the treatment in itself is stressful, we observed 10 d after the treatment some plants with dead buds (small yellow/white buds). Those plants for which the treatment had a toxic effect were eliminated from the analysis.

Pea Hydroponic Culture

The high-branching SL-deficient pea *rms1* mutant plant *rms1-10* was used. The nutrient solution (100%) was prepared by adding, in 1,000 L of water, the following macronutrients: HNO_3 (0.28 L), $(NH_4)_2HPO_4$ (120 g), $Ca(NO_3)_2$ (40 g), $Mg(NO_3)_2$ (140 g), KNO_3 (550 g), $(NH_4)_2MoO_4$ (0.05 g), H_3BO_3 (15 g), $MnSO_4 \cdot H_2O$ (2 g), $ZnSO_4 \cdot 0.7H_2O$ (1 g), $CuSO_4 \cdot 0.5H_2O$ (0.25 g), and Sequestrene (10 g; Fe-EDTA solution). Pea seeds were germinated in wet sand for 6 d. Germinated seeds were placed in premade holes in the lid (35 holes per lid, 20 mm diameter) of a hydroponic polyvinyl chloride opaque pot containing the hydroponic culture solution (47 L, pH 5.8). Acetone or the compound to be tested (dissolved in acetone) was added to the hydroponic culture solution to give a final concentration of 0, 1, or 3 μM of the compound to be tested and 0.01% acetone. The hydroponic culture solution was continuously aerated by an aquarium pump and was replaced weekly. Eight days after the beginning of the treatment, branch/lateral bud lengths (nodes 1–6) were measured with an electronic caliper.

PsBRC1 Transcript Levels

The different compounds were applied directly to the bud as done in branching bioassays. The axillary buds at node 3 from 30 plants per treatment and biological repeat were dissected. Axillary buds were harvested, total RNA was isolated and quantified, complementary DNA was synthesized, and real-time PCR gene expression analyses were conducted as described (Braun et al., 2012). Quantitative real-time PCR analyses were performed using SYBR ROX RealMasterMix (5Prime). Cycling conditions for amplification were 95°C for 10 min, 50 cycles of 95°C for 5 s, 62°C for 5 s, and 72°C for 15 s, followed by 0.1°C s^{-1} ramping up to 95°C for fusion curve characterization. Three biological repeats were analyzed in duplicate. To calculate relative transcript levels, the comparative cycle method based on nonequal efficiencies was used (Pfaffl, 2001). Transcript levels for the different genes were expressed relative to expression of the *EF1α* gene (Johnson et al., 2006). Primer sequences were as follows: PsBRC1 forward (5′-TCGAAAGACGGAATCAAACA-3′) and PsBRC1 reverse (5′-TCCCTTGCTCTTTCTCTTGC-3′); EF1α forward (5′-TGTGCCA-GTGGGACGTGTTG-3′) and EF1α reverse (5′-CTCGTGGTGCATCTCAACGG-3′).

Germination Stimulation Activity Assay

GR24 and SL analogs were resuspended in acetone at 10 mmol L^{-1} and then diluted with water at 1 mmol L^{-1} (water:acetone 99:1, v/v). Dilutions of 1 × 10^{-3} to 1 × 10^{-15} mol L^{-1} were then performed in water:acetone (99:1, v/v). Seeds of *Phelipanche ramosa* (from St. Martin de Fraigneau, France, 2005, on *Brassica napus*) were surface sterilized according to Dos Santos et al. (2003), resuspended in sterile water (10 g L^{-1}), and distributed on 96-well plates (50 μL, approximately 100 seeds per well). After preconditioning (7 d and 21°C, on a dark, sealed plate), GR24 (10×) or other molecules were added and volumes were adjusted to 100 μL with water (water:acetone 999:1, v/v). Controls were made with water:acetone (999:1, v/v) and without seeds. Plates were incubated for germination (21°C, in the dark). After 4 d, the germinated seeds were counted with a stereomicroscope (SZX10; Olympus). Seeds were considered as germinated when the radicle protruded out of the seed coat. Each germination assay was repeated at least three times. For each compound tested, dose-response curves [g = f(c), where g = germination percentage, f = function, and c = concentration (mol L^{-1})] and EC_{50} were modeled with a four-parameter logistic curve computed with SigmaPlot 10.0.

Statistical Analyses

Because deviations from normality were observed for axillary bud length after SL treatment, the Kruskal-Wallis test was used to assess the significance of treatment in comparison with the control treatment (0 nM) using R Commander version 1.7-3 (Fox, 2005; Tables I–VI).

Supplemental Data

The following materials are available in the online version of this article.

Supplemental Figure S1. Bioassay on bud outgrowth using hydroponic culture: comparison of the activity of GR24 and GR5.

Supplemental Figure S2. Dose-dependent activity of the SL analogs GR24 and GR5.

Supplemental Figure S3. Effect of different SLs (500 nM) on *PsBRC1* transcript levels in axillary buds at node 3 of *rms1* plants.

Supplemental Figure S4. Stimulatory activity of GR24, GR5, **23**, and **30** toward *P. ramosa* seed germination.

ACKNOWLEDGMENTS

Bayer CropScience is acknowledged for the supply of strigol, sorgolactone, and 5-deoxystrigol and K. Yoneyama for the supply of fabacyl acetate, orobanchol, and orobanchyl acetate. We thank S. Bonhomme and R. Beau for their comments on the manuscript.

Received March 22, 2012; accepted June 20, 2012; published June 21, 2012.

LITERATURE CITED

Adam W, Bialas J, Hadjiarapoglou L (1991) A convenient preparation of acetone solutions of dimethyldioxirane. Chem Ber **124:** 2377

Agusti J, Herold S, Schwarz M, Sanchez P, Ljung K, Dun EA, Brewer PB, Beveridge CA, Sieberer T, Sehr EM, Greb T (2011) Strigolactone signaling is required for auxin-dependent stimulation of secondary growth in plants. Proc Natl Acad Sci USA **108:** 20242–20247

Akiyama K, Hayashi H (2006) Strigolactones: chemical signals for fungal symbionts and parasitic weeds in plant roots. Ann Bot (Lond) **97:** 925–931

Akiyama K, Matsuzaki K, Hayashi H (2005) Plant sesquiterpenes induce hyphal branching in arbuscular mycorrhizal fungi. Nature **435:** 824–827

Akiyama K, Ogasawara S, Ito S, Hayashi H (2010) Structural requirements of strigolactones for hyphal branching in AM fungi. Plant Cell Physiol **51:** 1104–1117

Alder A, Jamil M, Marzorati M, Bruno M, Vermathen M, Bigler P, Ghisla S, Bouwmeester H, Beyer P, Al-Babili S (2012) The path from β-carotene to carlactone, a strigolactone-like plant hormone. Science **335:** 1348–1351

Antoniotti S, Duñach E (2008) Facile preparation of metallic triflates and triflimidates by oxidative dissolution of metal powders. Chem Commun (Camb) **44:** 993–995

Arite T, Umehara M, Ishikawa S, Hanada A, Maekawa M, Yamaguchi S, Kyozuka J (2009) d14, a strigolactone-insensitive mutant of rice, shows an accelerated outgrowth of tillers. Plant Cell Physiol **50:** 1416–1424

Besserer A, Puech-Pagès V, Kiefer P, Gomez-Roldan V, Jauneau A, Roy S, Portais JC, Roux C, Bécard G, Séjalon-Delmas N (2006) Strigolactones stimulate arbuscular mycorrhizal fungi by activating mitochondria. PLoS Biol **4:** e226

Beveridge CA (2000) Long-distance signalling and a mutational analysis of branching in pea. Plant Growth Regul **32:** 193–203

Beveridge CA, Kyozuka J (2010) New genes in the strigolactone-related shoot branching pathway. Curr Opin Plant Biol **13:** 34–39

Beveridge CA, Symons GM, Murfet IC, Ross JJ, Rameau C (1997) The rms1 mutant of pea has elevated indole-3-acetic acid levels and reduced root-sap zeatin riboside content but increased branching controlled by graft-transmissible signal(s). Plant Physiol **115:** 1251–1258

Booker J, Auldridge M, Wills S, McCarty D, Klee H, Leyser O (2004) MAX3/CCD7 is a carotenoid cleavage dioxygenase required for the synthesis of a novel plant signaling molecule. Curr Biol **14:** 1232–1238

Bouwmeester HJ, Roux C, Lopez-Raez JA, Bécard G (2007) Rhizosphere communication of plants, parasitic plants and AM fungi. Trends Plant Sci **12:** 224–230

Braun N, de Saint Germain A, Pillot JP, Boutet-Mercey S, Dalmais M, Antoniadi I, Li X, Maia-Grondard A, Le Signor C, Bouteiller N, et al (2012) The pea TCP transcription factor PsBRC1 acts downstream of strigolactones to control shoot branching. Plant Physiol **158:** 225–238

Brewer PB, Dun EA, Ferguson BJ, Rameau C, Beveridge CA (2009) Strigolactone acts downstream of auxin to regulate bud outgrowth in pea and Arabidopsis. Plant Physiol **150:** 482–493

Canevet JC, Graff Y (1978) Friedel-Crafts reaction of aromatic derivatives with 1,4-dicarbonyl-2,3-ethylenic compounds. II. Alkylations by some 5-hydroxy or 5-chloro-2,5-dihydro-2-furannones: new method for synthesis of 1h-indene-1-carboxylic acids. Tetrahedron **34:** 1935–1942

Chen VX, Boyer F-D, Rameau C, Retailleau P, Vors J-P, Beau J-M (2010) Stereochemistry, total synthesis, and biological evaluation of the new plant hormone solanacol. Chemistry **16:** 13941–13945

Cook CE, Coggon P, McPhail AT, Wall ME, Whichard LP, Egley GH, Luhan PA (1972) Germination stimulants. 2. Structure of strigol-potent seed germination stimulant for witchweed (Striga lutea Lour.). J Am Chem Soc **94:** 6198–6199

Cook CE, Whichard LP, Turner B, Wall ME, Egley GH (1966) Germination of witchweed (Striga lutea Lour.): isolation and properties of a potent stimulant. Science **154:** 1189–1190

Crawford S, Shinohara N, Sieberer T, Williamson L, George G, Hepworth J, Müller D, Domagalska MA, Leyser O (2010) Strigolactones enhance competition between shoot branches by dampening auxin transport. Development **137:** 2905–2913

Domagalska MA, Leyser O (2011) Signal integration in the control of shoot branching. Nat Rev Mol Cell Biol **12:** 211–221

Dos Santos CV, Letousey P, Delavault P, Thalouarn P (2003) Defense gene expression analysis of Arabidopsis thaliana parasitized by Orobanche ramosa. Phytopathology **93:** 451–457

Dun EA, de Saint Germain A, Rameau C, Beveridge CA (2012) Antagonistic action of strigolactone and cytokinin in bud outgrowth control. Plant Physiol **158:** 487–498

Fell SCM, Harbridge JB (1990) 2,5-Dimethoxy-2,5-dihydrofuran: a convenient synthon for a novel mono-protected glyoxal. Synthesis of 4-hydroxybutenolides. Tetrahedron Lett **31:** 4227–4228

Foo E, Davies NW (2011) Strigolactones promote nodulation in pea. Planta **234:** 1073–1081

Fox J (2005) The R commander: a basic-statistics graphical user interface to R. J Stat Softw **14:** 1–41

Fukui K, Ito S, Ueno K, Yamaguchi S, Kyozuka J, Asami T (2011) New branching inhibitors and their potential as strigolactone mimics in rice. Bioorg Med Chem Lett **21:** 4905–4908

Galloway WRJD, Hodgkinson JT, Bowden SD, Welch M, Spring DR (2011) Quorum sensing in gram-negative bacteria: small-molecule modulation of AHL and AI-2 quorum sensing pathways. Chem Rev **111:** 28–67

Gomez-Roldan V, Fermas S, Brewer PB, Puech-Pagès V, Dun EA, Pillot J-P, Letisse F, Matusova R, Danoun S, Portais J-C, et al (2008) Strigolactone inhibition of shoot branching. Nature **455:** 189–194

Gomez-Sanchez A, Moya PB, Bellanato J (1984) Protection of the amino group of amino-sugars by the acylvinyl group. Part I. Glycoside formation by the Fischer reaction. Carbohydr Res **135:** 101–116

Gould KS, Cutter EG, Young JPW, Charlton WA (1987) Positional differences in size, morphology, and in vitro performance of pea axillary buds. Can J Bot **65:** 406–411

Hoffmann HMR, Schmidt B, Wolff S (1989) Preparation of 5-bromotetronates [4-alkoxy-5-bromo-2(5h)-furanones] and a new concept for the synthesis of aflatoxins and related structure types: tributyltin hydride versus palladium-promoted intramolecular hydroarylation. Tetrahedron **45:** 6113–6126

Johnson AW, Gowda G, Hassanali A, Knox J, Monaco S, Razavi Z, Rosebery G (1981) The preparation of synthetic analogs of strigol. J Chem Soc Perkin Trans **1981:** 1734–1743

Johnson X, Brcich T, Dun EA, Goussot M, Haurogné K, Beveridge CA, Rameau C (2006) Branching genes are conserved across species: genes controlling a novel signal in pea are coregulated by other long-distance signals. Plant Physiol **142:** 1014–1026

Just G, Chung BY, Kim S, Rosebery G, Rossy P (1976) Reactions of oxygen and sulfur anions with oxazolidine and thiazolidine derivatives of 2-mesyloxymethylglyceraldehyde acetonide. Can J Chem **54:** 2089–2093

Kapulnik Y, Delaux P-M, Resnick N, Mayzlish-Gati E, Wininger S, Bhattacharya C, Séjalon-Delmas N, Combier J-P, Bécard G, Belausov E, et al (2011) Strigolactones affect lateral root formation and root-hair elongation in Arabidopsis. Planta **233:** 209–216

Kim HI, Xie XN, Kim HS, Chun JC, Yoneyama K, Nomura T, Takeuchi Y (2010) Structure-activity relationship of naturally occurring strigolactones in Orobanche minor seed germination stimulation. J Pestic Sci **35:** 344–347

Limberg G, Thiem J (1995) [beta]-Elimination of protected aldono-1,4-lactones as a general approach to the synthesis of 2-keto-3-deoxyaldonic acids containing four to six carbon atoms. Carbohydr Res **275:** 107–115

Macalpine GA, Raphael RA, Shaw A, Taylor AW, Wild HJ (1976) Synthesis of germination stimulant (+/−)-strigol. J Chem Soc Perkin Trans 1 410–416

Malik H, Kohlen W, Jamil M, Rutjes FPJT, Zwanenburg B (2011) Aromatic A-ring analogues of orobanchol, new germination stimulants for seeds of parasitic weeds. Org Biomol Chem **9:** 2286–2293

Malik H, Rutjes F, Zwanenburg B (2010) A new efficient synthesis of GR24 and dimethyl A-ring analogues, germinating agents for seeds of the parasitic weeds Striga and Orobanche spp. Tetrahedron **66:** 7198–7203

Mangnus EM, Dommerholt FJ, Dejong RLP, Zwanenburg B (1992) Improved synthesis of strigol analog Gr24 and evaluation of the biological activity of its diastereomers. J Agric Food Chem **40:** 1230–1235

Mangnus EM, Zwanenburg B (1992) Tentative molecular mechanism for germination stimulation of Striga and Orobanche seeds by strigol and its synthetic analogs. J Agric Food Chem **40:** 1066–1070

Matusova R, Rani K, Verstappen FWA, Franssen MCR, Beale MH, Bouwmeester HJ (2005) The strigolactone germination stimulants of the plant-parasitic *Striga* and *Orobanche* spp. are derived from the carotenoid pathway. Plant Physiol **139:** 920–934

Parniske M (2008) Arbuscular mycorrhiza: the mother of plant root endosymbioses. Nat Rev Microbiol **6:** 763–775

Pfaffl MW (2001) A new mathematical model for relative quantification in real-time RT-PCR. Nucleic Acids Res **29:** e45

Prandi C, Occhiato EG, Tabasso S, Bonfante P, Novero M, Scarpi D, Bova ME, Miletto I (2011) New potent fluorescent analogues of strigolactones: synthesis and biological activity in parasitic weed germination and fungal branching. Eur J Org Chem **2011:** 3781–3793

Proust H, Hoffmann B, Xie X, Yoneyama K, Schaefer DG, Yoneyama K, Nogué F, Rameau C (2011) Strigolactones regulate protonema branching and act as a quorum sensing-like signal in the moss Physcomitrella patens. Development **138:** 1531–1539

Rameau C, Bodelin C, Cadier D, Grandjean O, Miard F, Murfet IC (1997) New *ramosus* mutants at loci *Rms1, Rms3* and *Rms4* resulting from the mutation breeding program at Versailles. Pisum Genet **29:** 7–12

Rani K, Zwanenburg B, Sugimoto Y, Yoneyama K, Bouwmeester HJ (2008) Biosynthetic considerations could assist the structure elucidation of host plant produced rhizosphere signalling compounds (strigolactones) for arbuscular mycorrhizal fungi and parasitic plants. Plant Physiol Biochem **46:** 617–626

Reizelman A, Wigchert SCM, del-Bianco C, Zwanenburg B (2003) Synthesis and bioactivity of labelled germination stimulants for the isolation and identification of the strigolactone receptor. Org Biomol Chem **1:** 950–959

Ruyter-Spira C, Kohlen W, Charnikhova T, van Zeijl A, van Bezouwen L, de Ruijter N, Cardoso C, Lopez-Raez JA, Matusova R, Bours R, et al (2011) Physiological effects of the synthetic strigolactone analog GR24 on root system architecture in Arabidopsis: another belowground role for strigolactones? Plant Physiol **155:** 721–734

Sato D, Awad AA, Takeuchi Y, Yoneyama K (2005) Confirmation and quantification of strigolactones, germination stimulants for root parasitic plants Striga and Orobanche, produced by cotton. Biosci Biotechnol Biochem **69:** 98–102

Scaffidi A, Waters MT, Bond CS, Dixon KW, Smith SM, Ghisalberti EL, Flematti GR (2012) Exploring the molecular mechanism of karrikins and strigolactones. Bioorg Med Chem Lett **22:** 3743–3746

Schachtschabel D, Boland W (2007) Efficient generation of a trisporoid library by combination of synthesis and biotransformation. J Org Chem **72:** 1366–1372

Schreiber J, Wermuth CG (1965) Etude de la condensation de l'acide pyruvique avec les aldéhydes aliphatiques non substitués en alpha. I. Produits de condensation dont la chaine carbonée est ramifiée-semialdéhydes méthyl-alcoyl maliques et semialdéhydes méthyl-alcoyl maléiques. Bull Soc Chim Fr 2242–2249

Simon L, Bousquet J, Levesque RC, Lalonde M (1993) Origin and diversification of endomycorrhizal fungi and coincidence with vascular land plants. Nature **363:** 67–69

Sorefan K, Booker J, Haurogné K, Goussot M, Bainbridge K, Foo E, Chatfield S, Ward S, Beveridge C, Rameau C, et al (2003) MAX4 and RMS1 are orthologous dioxygenase-like genes that regulate shoot branching in Arabidopsis and pea. Genes Dev **17:** 1469–1474

Soto MJ, Fernandez-Aparicio M, Castellanos-Morales V, Garcia-Garrido JM, Ocampo JA, Delgado MJ, Vierheilig H (2010) First indications for the involvement of strigolactones on nodule formation in alfalfa (Medicago sativa). Soil Biol Biochem **42:** 383–385

Stévenin A, Boyer F-D, Beau J-M (2012) Highly selective formation of β-glycosides of N-acetylglucosamine using catalytic iron(III) triflate. Eur J Org Chem **2012:** 1699–1702

Surmont R, Verniest G, De Kimpe N (2010) Short synthesis of the seed germination inhibitor 3,4,5-trimethyl-2(5H)-furanone. J Org Chem **75:** 5750–5753

Thuring J, Keltjens R, Nefkens GHL, Zwanenburg B (1997) Synthesis and biological evaluation of potential substrates for the isolation of the strigol receptor. J Chem Soc Perkin Trans 1 759–765

Tsuchiya Y, McCourt P (2012) Strigolactones as small molecule communicators. Mol Biosyst **8:** 464–469

Tumlinson JH, Klein MG, Doolittle RE, Ladd TL, Proveaux AT (1977) Identification of the female Japanese beetle sex pheromone: inhibition of male response by an enantiomer. Science **197:** 789–792

Turnbull CGN, Booker JP, Leyser HMO (2002) Micrografting techniques for testing long-distance signalling in Arabidopsis. Plant J **32:** 255–262

Ueno K, Fujiwara M, Nomura S, Mizutani M, Sasaki M, Takikawa H, Sugimoto Y (2011a) Structural requirements of strigolactones for germination induction of Striga gesnerioides seeds. J Agric Food Chem **59:** 9226–9231

Ueno K, Nomura S, Muranaka S, Mizutani M, Takikawa H, Sugimoto Y (2011b) Ent-2′-epi-orobanchol and its acetate, as germination stimulants for Striga gesnerioides seeds isolated from cowpea and red clover. J Agric Food Chem **59:** 10485–10490

Umehara M, Hanada A, Yoshida S, Akiyama K, Arite T, Takeda-Kamiya N, Magome H, Kamiya Y, Shirasu K, Yoneyama K, et al (2008) Inhibition of shoot branching by new terpenoid plant hormones. Nature **455:** 195–200

Vurro M, Yoneyama K (2012) Strigolactones: intriguing biologically active compounds. Perspectives for deciphering their biological role and for proposing practical application. Pest Manag Sci **68:** 664–668

Wolff S, Hoffmann HMR (1988) Aflatoxins revisited: convergent synthesis of the ABC moiety. Synthesis 760–763

Xie X, Kusumoto D, Takeuchi Y, Yoneyama K, Yamada Y, Yoneyama K (2007) 2′-Epi-orobanchol and solanacol, two unique strigolactones, germination stimulants for root parasitic weeds, produced by tobacco. J Agric Food Chem **55:** 8067–8072

Xie X, Yoneyama K, Kusumoto D, Yamada Y, Yokota T, Takeuchi Y, Yoneyama K (2008) Isolation and identification of alectrol as (+)-orobanchyl acetate, a germination stimulant for root parasitic plants. Phytochemistry **69:** 427–431

Xie XN, Yoneyama K (2010) The strigolactone story. Annu Rev Phytopathol **48:** 93–117

Xie XN, Yoneyama K, Harada Y, Fusegi N, Yamada Y, Ito S, Yokota T, Takeuchi Y, Yoneyama K (2009) Fabacyl acetate, a germination stimulant for root parasitic plants from Pisum sativum. Phytochemistry **70:** 211–215

Yamaguchi S, Umehara M, Akiyama K, inventors. December 2, 2010. Plant branching inhibitor, method for producing same, and plant branching inhibitory composition. Japan Patent Application No. WO/2010/137662

Yoneyama K, Awad AA, Xie XN, Yoneyama K, Takeuchi Y (2010) Strigolactones as germination stimulants for root parasitic plants. Plant Cell Physiol **51:** 1095–1103

Yoneyama K, Xie X, Kim HI, Kisugi T, Nomura T, Sekimoto H, Yokota T, Yoneyama K (2012) How do nitrogen and phosphorus deficiencies affect strigolactone production and exudation? Planta **235:** 1197–1207

Yoneyama K, Xie X, Yoneyama K, Takeuchi Y (2009) Strigolactones: structures and biological activities. Pest Manag Sci **65:** 467–470

Yoneyama K, Xie XN, Kusumoto D, Sekimoto H, Sugimoto Y, Takeuchi Y, Yoneyama K (2007) Nitrogen deficiency as well as phosphorus deficiency in sorghum promotes the production and exudation of 5-deoxystrigol, the host recognition signal for arbuscular mycorrhizal fungi and root parasites. Planta **227:** 125–132

Zanatta N, Barichello R, Pauletto MM, Bonacorso HG, Martins MAP (2003) Convenient synthesis of 3-aminomethylenedihydrofuran-2-ones. Tetrahedron Lett **44:** 961–964

Zwanenburg B, Mwakaboko AS (2011) Strigolactone analogues and mimics derived from phthalimide, saccharine, p-tolylmalondialdehyde, benzoic and salicylic acid as scaffolds. Bioorg Med Chem **19:** 7394–7400

Zwanenburg B, Mwakaboko AS, Reizelman A, Anilkumar G, Sethumadhavan D (2009) Structure and function of natural and synthetic signalling molecules in parasitic weed germination. Pest Manag Sci **65:** 478–491